

Perturbative QCD for Beginners

Basics of Colour Dynamics and QCD Parton Evolution

Yuri L. Dokshitzer (yuri@lpthe.jussieu.fr)

LPTHE, Université Paris-VI, 4 Place Jussieu, Paris

Abstract. In these lectures we first review an experimental evidence in favour of small-distance quark-gluon dynamics as the basis for multiple hadron production in hard interactions. Then, we discuss the basics of QCD parton picture. The emphasis is given to the rôle of gluon coherence effects both in space- and time-like evolution.

Keywords: perturbative QCD, multiple hadroproduction

1. Preface

Our field has emerged as a result of the digression: *natural philosophy* \rightarrow *physics* \rightarrow *quantum physics* \rightarrow *elementary particle physics*. The older generation participated in specifying *elementary particle physics* \rightarrow *high energy physics*. In the past 20 years, with an advent of Quantum Chromodynamics, we have witnessed the final step after which QCD has acquired its today's split personality: *high energy physics* \rightarrow *soft physics* + *hard physics*. Both “*hard*” and “*soft*” are hard subjects, and the softer the harder.

Until recently QCD studies were concentrated on small-distance phenomena, observables and characteristics that are as insensitive to large-distance confinement physics as possible. This is the realm of “hard processes” in which a large momentum transfer Q^2 , either time-like $Q^2 \gg 1 \text{ GeV}^2$, or space-like $Q^2 \ll -1 \text{ GeV}^2$, is applied to hadrons in order to probe their small-distance quark-gluon structure.

Perturbative QCD (pQCD) controls the relevant cross sections and, to a lesser extent, the structure of final states produced in hard interactions. Whatever the hardness of the process, it is hadrons, not quarks and gluons, that hit the detectors. For this reason alone, the applicability of the pQCD approach, even to hard processes, is far from being obvious. One has to rely on plausible arguments (completeness, duality) and look for observables that are *less vulnerable* towards our ignorance about confinement.

To give an example, we cannot deduce from the first principles parton distributions inside hadrons (PDF, or structure functions). However, the rate of their $\ln Q^2$ -dependence (scaling violation) is an example of a Collinear-and-Infrared-Safe (CIS) measure and stays under pQCD jurisdiction.



© 2001 Kluwer Academic Publishers. Printed in the Netherlands.

Speaking about the final state structure, we cannot predict, say, the kaon multiplicity or the pion energy spectrum. However, one can decide to be not too picky and concentrate on global characteristics of the final states rather than on the yield of specific hadrons. Being sufficiently inclusive with respect to final hadron species, one can rely on a picture of the energy-momentum flow in hard collisions supplied by pQCD — the jet pattern.

There are well elaborated procedures for counting jets (CIS jet finding algorithms) and for quantifying the internal structure of jets (CIS jet shape variables). They allow the study of the gross features of the final states while staying away from the physics of hadronisation. Along these lines one visualizes asymptotic freedom, checks out gluon spin and colour, predicts and verifies scaling violation pattern in hard cross sections, etc. These and similar checks have constituted the basic QCD tests of the past two decades.

This epoch is over. Now the High Energy Particle physics community is trying to probe genuine confinement effects in hard processes to learn more about strong interactions. The programme is ambitious and provocative. Friendly phenomenology keeps it afloat and feeds our hopes of extracting valuable information about physics of hadronisation.

2. Bremsstrahlung gluons at work

High-energy annihilation $e^+e^- \rightarrow$ hadrons, deep inelastic lepton-hadron scattering (DIS), production in hadron-hadron collisions of massive lepton pairs, heavy quarks and their bound states, large transverse momentum jets and photons are classical examples of hard processes.

Copious production of hadrons is typical for all these processes. On the other hand, at the microscopic level, multiple quark-gluon “production” is to be expected as a result of QCD bremsstrahlung — gluon radiation accompanying abrupt creation/scattering of colour partons.

Is there a correspondence between observable hadron and calculable quark-gluon production?

2.1. SCALING VIOLATION PATTERN

An indirect evidence that gluons are there, and that they behave, can be obtained from the study of the scaling violation pattern. QCD quarks (and gluons) are not point-like particles, as the orthodox parton model once assumed. Each of them is surrounded by a proper field coat — a coherent virtual cloud consisting of gluons and “sea” $q\bar{q}$ pairs.

A hard probe applied to such a dressed parton breaks coherence of the cloud. Constituents of these field fluctuations are then released as particles accompanying the hard interaction. The harder the hit, the larger an intensity of bremsstrahlung and, therefore, the fraction of the energy-momentum of the dressed parton that the bremsstrahlung quanta typically carry away. Thus we should expect, in particular, that the probability that a “bare” core quark carries a large fraction of the energy of its dressed parent will decrease with increase of Q^2 . And so it does.

The logarithmic scaling violation pattern in DIS structure functions is well established and meticulously follows the QCD prediction based on the parton evolution picture.

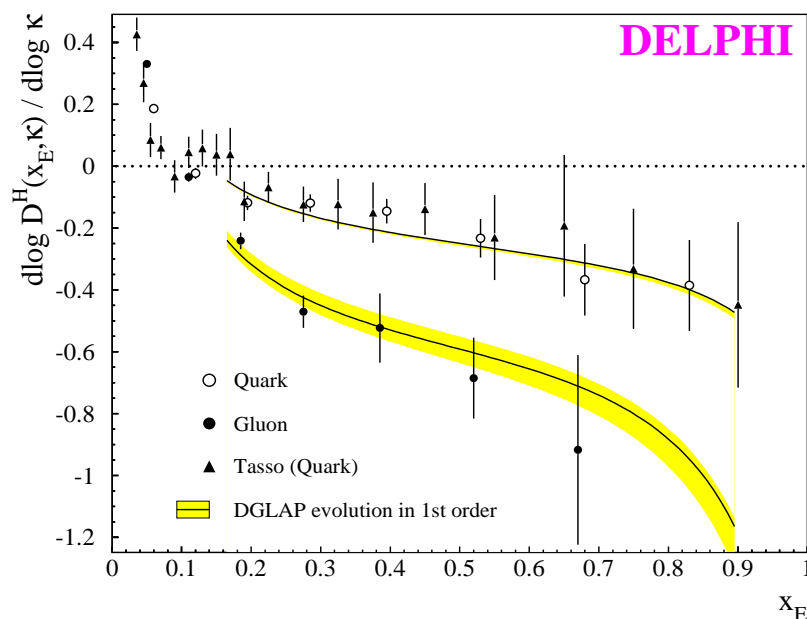


Figure 1. Scaling violation rates in inclusive hadron distributions from gluon and quark jets (Abreu et al., 1999)

In DIS we look for a “bare” quark inside a target dressed one. In e^+e^- hadron annihilation at large energy $s = Q^2$ the chain of events is reversed. Here we produce instead a bare quark with energy $Q/2$, which then “dresses up”. In the process of restoring its proper field-coat our parton produces (a controllable amount of) bremsstrahlung radiation which leads to formation of a hadron jet. Having done so, in the end of the day it becomes a constituent of one of the hadrons that hit the detector. Typically, this is the leading hadron. However, the fraction x_E of the initial energy $Q/2$ that is left to the leader depends on the

amount of accompanying radiation and, therefore, on Q^2 (the larger, the smaller). In fact, the same rule (and the same formula) applies to the scaling violation pattern in e^+e^- fragmentation functions (time-like parton evolution) as to that in the DIS parton distributions (space-like evolution).

What makes the annihilation channel particularly interesting, is that the present day experiments are so sophisticated that they provide us with a near-to-perfect separation between quark- and gluon-initiated jets (the latter being extracted from heavy-quark-tagged three-jet events).

In Fig. 1 a comparison is shown of the scaling violation rates in the hadron spectra from gluon and quark jets, as a function of the hardness scale κ that characterizes a given jet (Abreu et al., 1999). For large values of $x_E \sim 1$ the ratio of the logarithmic derivatives is predicted to be close to that of the gluon and quark ‘‘colour charges’’, $C_A/C_F = 9/4$. Experimentally, the ratio is measured to be

$$\frac{C_A}{C_F} = 2.23 \pm 0.09_{\text{stat.}} \pm 0.06_{\text{syst.}} \quad (1)$$

2.2. BREMSSTRAHLUNG PARTON AND HADRON MULTIPLICITIES

Since accompanying QCD radiation seems to be there, we can make a step forward by asking for a *direct* evidence: what is the fate of those gluons and sea quark pairs produced via multiple initial gluon bremsstrahlung followed by parton multiplication cascades? Let us look at the Q -dependence of the mean hadron multiplicity, the quantity dominated by relatively soft particles with $x_E \ll 1$. This is the kinematical region populated by accompanying QCD radiation.

Fig. 2 demonstrates that the hadron multiplicity increases with the hardness of the jet proportional to the multiplicity of secondary gluons and sea quarks. The ratio of the slopes, once again, provides an independent measure of the ratio of the colour charges, which is consistent with (1) (Abreu et al., 1999):

$$\frac{C_A}{C_F} = 2.246 \pm 0.062_{\text{stat.}} \pm 0.008_{\text{syst.}} \pm 0.095_{\text{theo.}} \quad (2)$$

2.3. INCLUSIVE HADRON DISTRIBUTION IN JETS

Since the total numbers match, it is time to ask a more delicate question about energy-momentum distribution of final hadrons versus that of the underlying parton ensemble. One should not be too picky in addressing such a question. It is clear that hadron-hadron correlations,

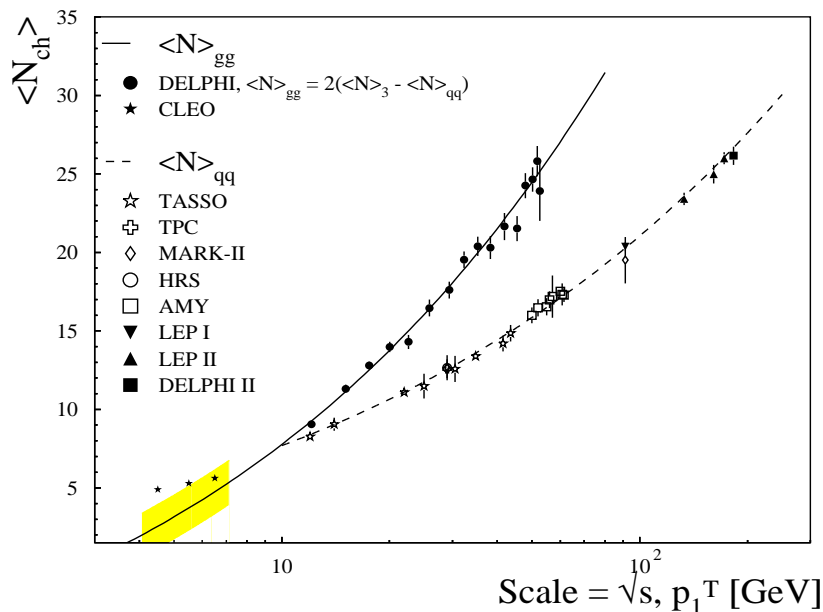


Figure 2. Charged hadron multiplicities in gluon and quark jets (Abreu et al., 1999).

for example, will show resonant structures about which the quark-gluon speaking pQCD can say little, if anything, at the present state of the art. Inclusive single-particle distributions, however, have a better chance to be closely related. Triggering a single hadron in the detector, and a single parton on paper, one may compare the structure of the two distributions to learn about dynamics of hadronisation.

Inclusive energy spectrum of soft bremsstrahlung partons in QCD jets has been derived in 1984 in the so-called MLLA — the Modified Leading Logarithmic Approximation (Dokshitzer&Troyan, Mueller). This approximation takes into account all essential ingredients of parton multiplication in the next-to-leading order. They are: parton splitting functions responsible for the energy balance in parton splitting, the running coupling $\alpha_s(k_1^2)$ depending on the relative transverse momentum of the two offspring and exact angular ordering. The latter is a consequence of soft gluon coherence and plays, as we shall discuss below, an essential rôle in parton dynamics. In particular, gluon coherence suppresses multiple production of very small momentum gluons. It is particles with intermediate energies that multiply most efficiently. As a result, the energy spectrum of relatively soft secondary partons in jets acquires a characteristic hump-backed shape. The position of

the maximum in the logarithmic variable $\xi = -\ln x$, the width of the hump and its height increase with Q^2 in a predictable way.

The shape of the inclusive spectrum of all charged hadrons (dominated by π^\pm) exhibits the same features. This comparison, pioneered by Glen Cowan (ALEPH) and the OPAL collaboration, has later become a standard test of analytic QCD predictions. First scrutinized at LEP, the similarity of parton and hadron energy distributions has been verified at SLC and KEK e^+e^- machines, as well as at HERA and Tevatron where hadron jets originate not from bare quarks dug up from the vacuum by a highly virtual photon/ Z^0 but from hard partons kicked out from initial hadron(s).

In Fig. 3 (DELPHI) the comparison is made of the all-charged hadron spectra at various annihilation energies Q with the so-called “distorted Gaussian” fit (Fong & Webber 1989) which employs the first four moments (the mean, width, skewness and kurtosis) of the MLLA distribution around its maximum.

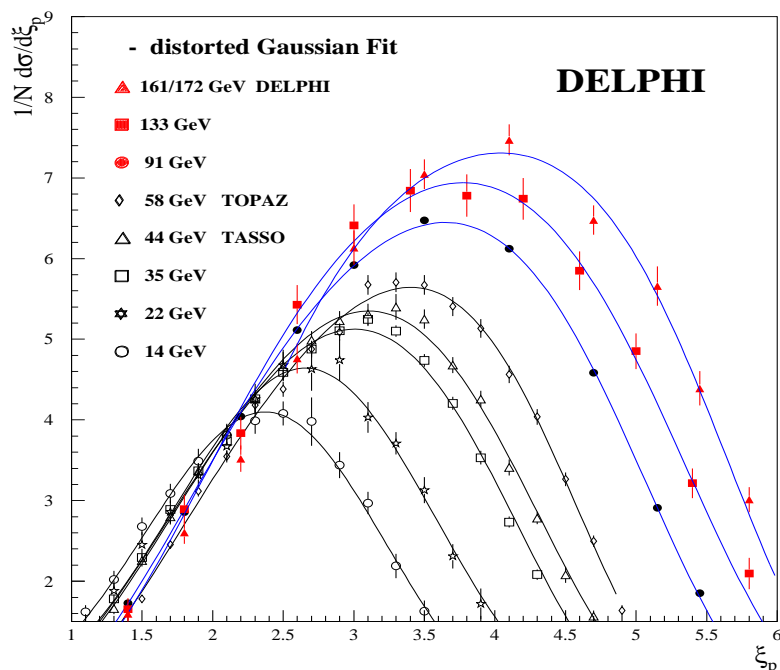


Figure 3. Inclusive energy distribution of charged hadrons in jets produced in e^+e^- annihilation

Shall we say, a (routine, interesting, wonderful) check of yet another QCD prediction? Better not. Such a close similarity offers a deep puzzle, even a worry, rather than a successful test. Indeed, after a little exercise

in translating the values of the logarithmic variable $\xi = \ln(E_{\text{jet}}/p)$ in Fig. 3 into GeVs you will see that the actual hadron momenta at the maxima are, for example, $p = \frac{1}{2}Q \cdot e^{-\xi_{\text{max}}} \simeq 0.42, 0.85$ and 1.0 GeV for $Q=14, 35$ GeV and at LEP-1, $Q=91$ GeV. Is it not surprising that the pQCD spectrum is mirrored by that of the pions (which constitute 90% of all charged hadrons produced in jets) with momenta well below 1 GeV?!

For this very reason the observation of the parton-hadron similarity was initially met with a serious and well grounded skepticism: it looked more natural (and was more comfortable) to blame the finite hadron mass effects for fall-off of the spectrum at large ξ (small momenta) rather than seriously believe in applicability of the pQCD consideration down to such disturbingly small momentum scales.

This worry has been recently answered. Andrey Korytov (CDF) was the first to hear a theoretical suggestion (Dokshitzer et al., 1988) and carry out a study of the energy distribution of hadrons produced inside a restricted angular cone Θ around the jet axis. Theoretically, it is not the energy of the jet but the maximal parton transverse momentum inside it, $k_{\perp\text{max}} \simeq E_{\text{jet}} \sin \frac{\Theta}{2}$, that determines the hardness scale and thus the yield and the distribution of the accompanying radiation.

This means that by choosing a small opening angle one can study relatively small hardness scales but in a cleaner environment: due to the Lorentz boost effect, eventually all particles that form a short small- Q^2 QCD “hump” are now relativistic and concentrated at the tip of the jet.

For example, selecting hadrons inside a cone $\Theta \simeq 0.14$ around an energetic quark jet with $E_{\text{jet}} \simeq 100$ GeV (LEP-2) one should see that very “dubious” $Q = 14$ GeV curve in Fig. 3 but now with the maximum boosted from 0.45 GeV into a comfortable 6 GeV range.

In the CDF Fig. 4 (Korytov, 1996, Goulianos, 1997, Safonov, 1999) a close similarity between the hadron yield and the full MLLA parton spectra can no longer be considered accidental and be attributed to non-relativistic kinematical effects.

2.4. BRAVE GLUON COUNTING

Modulo Λ_{QCD} , there is only one unknown in this comparison, namely, the overall normalisation of the spectrum of hadrons relative to that of partons (bremsstrahlung gluons).

Strictly speaking, there should/could have been another free parameter, the one which quantifies one’s bravery in applying the pQCD dynamics. It is the minimal transverse momentum cutoff in parton cascades, $k_{\perp} > Q_0$. The strength of successive $1 \rightarrow 2$ parton splittings

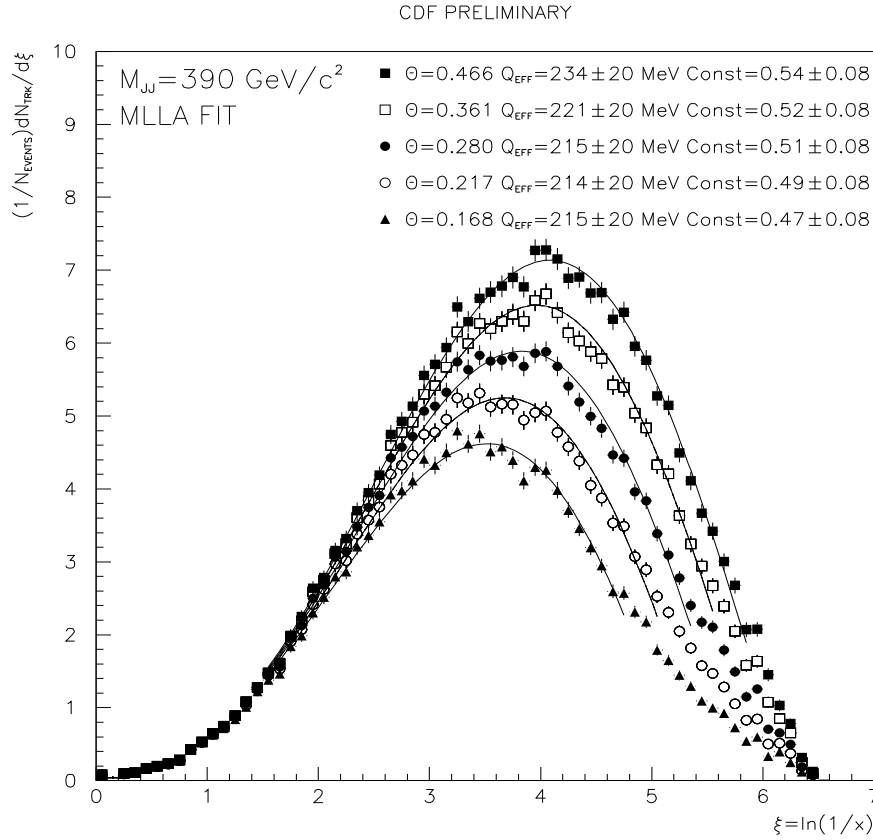


Figure 4. Inclusive energy distribution of charged hadrons in large- p_{\perp} jets (Goulianos, 1997).

is proportional to $\alpha_s(k_{\perp}^2)$ and grows with k_{\perp} decreasing. The necessity to terminate the process at some low transverse momentum scale where the PT coupling becomes large (and eventually hits the formal “Landau pole” at $k_{\perp} = \Lambda_{\text{QCD}}$) seems imminent. Surprisingly enough, it is not.

Believe it or not, the inclusive parton energy distribution turns out to be a CIS QCD prediction. Its crazy $Q_0 = \Lambda_{\text{QCD}}$ limit (the so-called “limiting spectrum”) is shown by solid curves in Fig. 4.

Choosing the minimal value for the collinear parton cutoff Q_0 can be looked upon as shifting, as far as possible, responsibility for particle multiplication in jets to the PT dynamics. This brave choice can be said to be dictated by experiment, in a certain sense. Indeed, with increase of Q_0 the parton parton distributions *stiffen* (parton energies are limited from below by the kinematical inequality $x E_{\text{jet}} \equiv k \geq k_{\perp} > Q_0$). The maxima would move to larger x (smaller ξ), departing from the data.

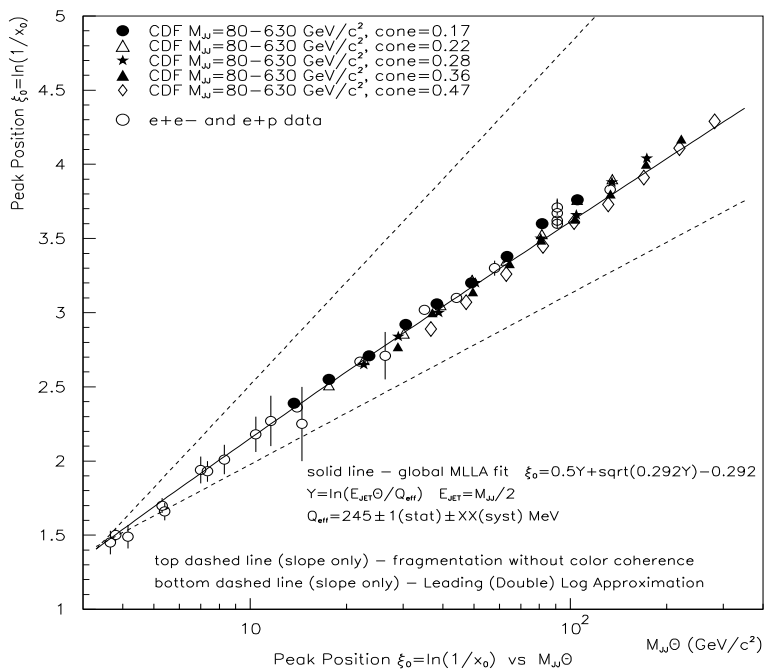


Figure 5. The position of the maximum versus the analytic MLLA prediction (Safonov, 1999).

A clean test of “brave gluon counting” is provided by Fig. 5 where the position of the hump, which is insensitive to the overall normalisation, is compared with the parameter-free MLLA pQCD prediction (Safonov, 1999).

To put a long story short, decreasing Q_0 we start to lose control of the interaction intensity of a parton with a given x and $k_\perp \sim Q_0$ (and thus may err in the overall production rate). However, such partons do not branch any further, do not produce any soft offspring, so that the *shape* of the resulting energy distribution remains undamaged. Colour coherence plays here a crucial rôle.¹

It is important to realize that knowing the spectrum of *partons*, even knowing it to be a CIS quantity in certain sense, does not guarantee on its own the predictability of the *hadron* spectrum. It is easy to imagine a world in which each quark and gluon with energy k produced at the small-distance stage of the process would have dragged behind its personal “string” giving birth to $\ln k$ hadrons in the final state (the

¹ A formal explanation of the tolerance of the *shape* of inclusive parton spectra to the dangerous small- k_\perp domain will be given below in Sec. 4.4.

Feynman plateau). The hadron yield then would be given by a convolution of the parton distribution with a logarithmic energy distribution of hadrons from the parton fragmentation.

If it were the case, each parton would have contributed to the yield of non-relativistic hadrons and the hadron spectra would peak at much smaller energies, $\xi_{\max} \simeq \ln Q$, in a spectacular difference with experiment.

Physically, it could be possible if the non-perturbative (NP) hadronisation physics did not respect the basic rule of the perturbative dynamics, namely, that of colour coherence.

There is nothing wrong with the idea of convoluting time-like parton production in jets with the inclusive NP parton→hadron fragmentation function, the procedure which is similar to convoluting space-like parton cascades with the NP initial parton distributions in a target proton to describe DIS structure functions.

What the nature is telling us, however, is that this NP fragmentation has a finite multiplicity and is *local* in the momentum space. Similar to its PT counterpart, the NP dynamics has a short memory: the NP conversion of partons into hadrons occurs locally in the configuration space.

In spite of a known similarity between the space- and time-like parton evolution pictures ($x \sim 1$), there is an essential difference between *small- x* physics of DIS structure functions and the jet fragmentation. In the case of the space-like evolution, in the limit of small Bjorken- x the problem becomes essentially non-perturbative and pQCD loses control of the DIS cross sections (Mueller, 1997, Camici&Ciafaloni, 1997). On the contrary, studying small Feynman- x particles originating from the time-like evolution of jets offers a gift and a puzzle: all the richness of the confinement dynamics reduces to a mere overall normalisation constant.

The fact that even a legitimate finite smearing due to hadronisation effects does not look mandatory makes one think of a deep duality between the hadron and quark-gluon languages applied to such a global characteristic of multihadron production as an inclusive energy spectrum.

The message is, that “brave gluon counting”, that is applying the pQCD language all the way down to very small transverse momentum scales, indeed reproduces the x - and Q -dependence of the observed inclusive energy spectra of charged hadrons (pions) in jets.

Even such a tiny effect as an envisaged difference in the position of the maxima in quark- and gluon-initiated humps (Fong&Webber, 1991) has been verified, 15 years later, by DELPHI (Hamacher et al., 1999).

Put together, the ideas behind the brave gluon counting are known as the hypothesis of Local Parton-Hadron Duality (Dokshitzer&Troyan, 1984). Experimental evidence in favour of LPHD is mounting, and so is list of challenging questions to be answered by the future quantitative theory of colour confinement.

2.5. QCD RADIOPHYSICS

Even more striking is *miraculously* successful rôle of gluons in predicting the pattern of hadron multiplicity flows in the inter-jet regions — realm of various *string/drag* effects. This is another class of multi-hadron production phenomena speaking in favour of LPHD. It deals with particle flows in the angular regions *between jets* in various multi-jet configurations. These particles do not belong to any particular jet, and their production, at the pQCD level, is governed by *coherent* soft gluon radiation off the multi-jet system as a whole. The ratios of particle (gluon) flows in different inter-jet valleys are given by parameter-free pQCD predictions and reveal the so-called “string” or “drag” effects. For a given kinematical jet configuration such ratios depend only on the number of colours (N_c).

It isn't strange at all that with *gluons* one can get, e.g., $1 + 1 = 2$ while $1 + 1 + 9/4 = 7/16$, which is a simple *radiophysics* of composite antennas, or *quantum mechanics* of conserved colour charges.

This particular example of “quantum arithmetics” has to do with comparison of hadron flows in the inter-quark valleys in $q\bar{q}\gamma$ and $q\bar{q}g$ (3-jet) events. The first equation describes the density of soft gluon radiation produced by two quarks in a $q\bar{q}\gamma$ event, with 1 standing for the colour quark charge.

Replacing the colour-blind photon by a gluon one gets an additional emitter with the relative strength $9/4$, as shown in the l.h.s. of the second equation. The resulting soft gluon yield in the $q\bar{q}$ direction, however, *decreases* substantially as a result of destructive interference between three elements of a composite colour antenna. In Fig. 6 the OPAL measurements are compared with the parameter-free theoretical prediction (Azimov et al., 1985).

Another example is the ratio of the multiplicity flow between a quark (antiquark) and a gluon to that in the $q\bar{q}$ valley in symmetric (“Mercedes”) three-jet $q\bar{q}g$ e^+e^- annihilation events:

$$\frac{dN_{q\bar{q}g}^{(q\bar{q}g)}}{dN_{q\bar{q}}^{(q\bar{q}g)}} \simeq \frac{5N_c^2 - 1}{2N_c^2 - 4} = \frac{22}{7}. \quad (3)$$

Emitting an energetic gluon off the initial quark pair depletes accompanying radiation in the backward direction: colour is *dragged* out of

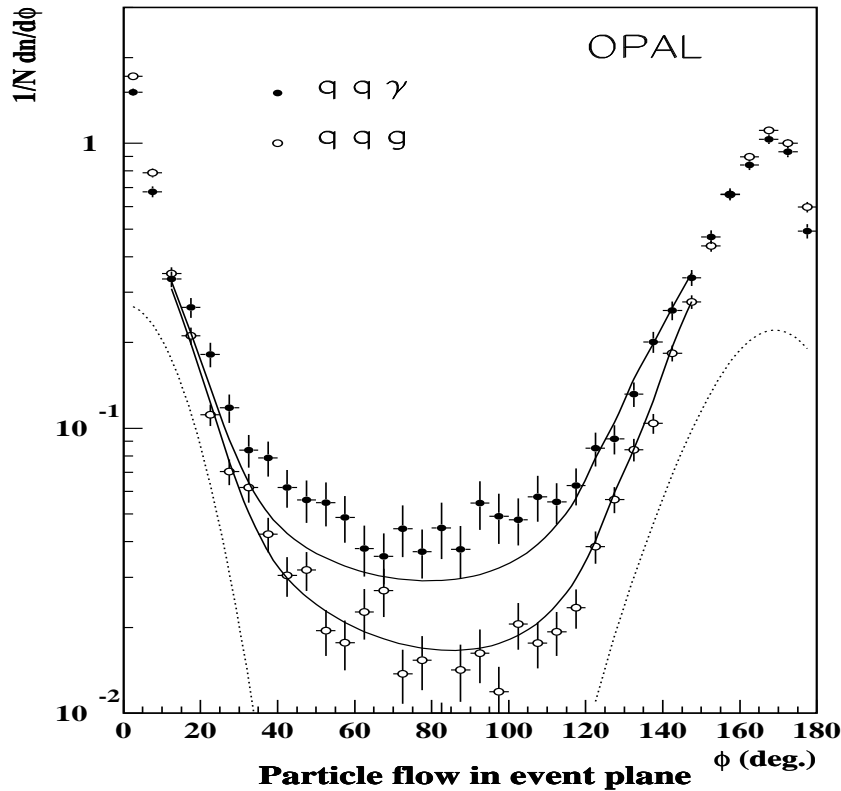


Figure 6. Comparison of particle flows in the $q\bar{q}$ valley in $q\bar{q}\gamma$ and $q\bar{q}g$ 3-jet events versus a parameter-free analytic prediction based on the soft gluon radiation pattern. (Akers et al., 1995)

the $q\bar{q}$ valley. This destructive interference effect is so strong that the resulting multiplicity flow falls below that in the least favourable direction *transversal* to the three-jet event plane. For symmetric “Mercedes” events the expected ratio is

$$\frac{dN_{\perp}^{(q\bar{q}\gamma)}}{dN_{q\bar{q}}^{(q\bar{q}g)}} \simeq \frac{N_C + 2C_F}{2(4C_F - N_C)} = \frac{17}{14}, \quad (4)$$

and tends to unity, in a predictable way, when the $q\bar{q}g$ ensemble becomes two-jet-like (Khoze et al., 1997). The *hadron* flow has been found, once again, to obediently follow that of coherent soft gluon radiation (DELPHI, 1999).

Nothing particularly strange, you might say. At the level of the PT accompanying gluon radiation (QCD radiophysics) such predictions are quite simple and straightforward to derive. Moreover, these predictions

are quite robust since, due to QCD coherence, the inter-jet gluon radiation is insensitive to internal structure of underlying jets. The only thing that matters is the colour topology of the primary system of hard partons and their kinematics.

What is rather strange, though, is that these and many similar numbers are being seen experimentally. The inter-jet particle flows we are discussing are dominated, at present energies, by very soft pions with typical momenta in the 100–300 MeV range! The fact that even such soft junk follows the pQCD rules is truly amazing.

What the nature seems to be telling us, is that

- The *colour field* that an ensemble of hard primary **partons** (parton antenna) develops, determines, on the one-to-one basis, the structure of final flows of **hadrons**.
- The Poynting vector of the colour field gets translated into the hadron Poynting vector without any visible reshuffling of particle momenta at the “hadronisation stage”.

When viewed *globally*, confinement is about *renaming* a flying-away quark into a flying-away pion rather than about forces *pulling* quarks together.

3. Basics of parton multiplication

In this lecture we shall recall the basic properties of accompanying radiation. The gluon bremsstrahlung (off quarks and gluons) is not much different from the photon emission off electric charges. So, we shall start from the electromagnetic radiation and turn to gluons later.

3.1. PHOTON BREMSSTRAHLUNG

Let us consider photon bremsstrahlung induced by a charged particle (electron) which scatters off an external field (e.g., a static electromagnetic field). The derivation is included in every textbook on QED, so we confine ourselves to the essential aspects.

The lowest order Feynman diagrams for photon radiation are depicted in Fig. 7, where p_1, p_2 are the momenta of the incoming and outgoing electron respectively and k represents the momentum of the emitted photon. The corresponding amplitudes, according to the Feynman rules, are given in momentum space by

$$M_i^\mu = e \bar{u}(p_2, s_2) V(p_2 + k - p_1) \frac{m + \not{p}_1 - \not{k}}{m^2 - (p_1 - k)^2} \gamma^\mu u(p_1, s_1), \quad (3.5a)$$

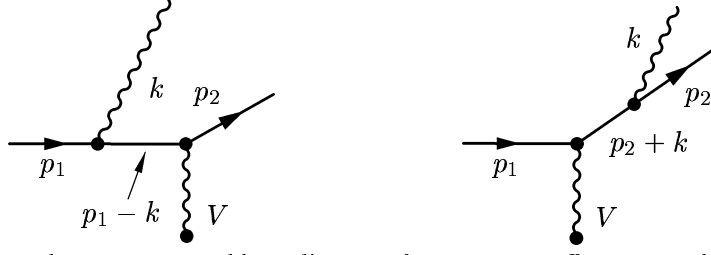


Figure 7. Photon Bremsstrahlung diagrams for scattering off an external field.

$$M_f^\mu = e \bar{u}(p_2, s_2) \gamma^\mu \frac{m + \not{p}_2 + \not{k}}{m^2 - (p_2 + k)^2} V(p_2 + k - p_1) u(p_1, s_1). \quad (3.5b)$$

Here V stands for the basic interaction amplitude which may depend in general on the momentum transfer (for the case of scattering off the static e.m. field, $V = \gamma^0$).

First we apply the soft-photon approximation, $\omega \ll p_1^0, p_2^0$, to neglect \not{k} terms in the numerators. To deal with the remaining matrix structure in the numerators of (3.5) we use the identity $\not{p} \gamma^\mu = -\gamma^\mu \not{p} + 2p^\mu$ and the Dirac equation for the on-mass-shell electrons,

$$\begin{aligned} (m + \not{p}_1) \gamma^\mu u(p_1) &= (2p_1^\mu + [(m - \not{p}_1)]) u(p_1) = 2p_1^\mu u(p_1), \\ \bar{u}(p_2) \gamma^\nu (m + \not{p}_2) &= \bar{u}(p_2) ([(m - \not{p}_2) + 2p_2^\nu] = 2p_2^\nu \bar{u}(p_2). \end{aligned}$$

Denominators for real electrons ($p_i^2 = m^2$) and the photon ($k^2 = 0$) become $m^2 - (p_1 - k)^2 = 2(p_1 k)$ and $m^2 - (p_2 + k)^2 = -2(p_2 k)$, so that for the total amplitude we obtain the factorized expression

$$M^\mu = e j^\mu \times M_{\text{el}}. \quad (3.6a)$$

Here M_{el} is the Born matrix element for non-radiative (elastic) scattering,

$$M_{\text{el}} = \bar{u}(p_2, s_2) V(p_2 - p_1) u(p_1, s_1) \quad (3.6b)$$

(in which the photon recoil effect has been neglected, $q = p_2 + k - p_1 \simeq p_2 - p_1$), and j^μ is the *soft accompanying radiation current*

$$j^\mu(k) = \frac{p_1^\mu}{(p_1 k)} - \frac{p_2^\mu}{(p_2 k)}. \quad (3.6c)$$

Factorisation (3.6a) is of the most general nature. The form of j^μ does not depend on the details of the underlying process, neither on the nature of participating charges (electron spin, in particular). The only thing which matters is the momenta and charges of incoming and outgoing particles. Generalization to an arbitrary process is straightforward

and results in assembling the contributions due to all initial and final particles, weighted with their respective charges.

The soft current (3.6c) has a classical nature. It can be derived from the classical electrodynamics by considering the potential induced by change of the e.m. current due to scattering.

3.2. SOFT RADIATION CROSS SECTION

To calculate the radiation probability we square the amplitude projected onto a photon polarization state ϵ_μ^λ , sum over λ and supply the photon phase space factor to write down

$$dW = e^2 \sum_{\lambda=1,2} \left| \epsilon_\mu^\lambda j^\mu \right|^2 \frac{\omega^2 d\omega d\Omega_\gamma}{2\omega (2\pi)^3} dW_{\text{el}} . \quad (3.7)$$

The sum runs over two physical polarization states of the real photon, described by normalized polarization vectors orthogonal to its momentum:

$$\epsilon_\lambda^\mu(k) \cdot \epsilon_{\mu,\lambda'}^*(k) = -\delta_{\lambda\lambda'} , \quad \epsilon_\lambda^\mu(k) \cdot k_\mu = 0 ; \quad \lambda, \lambda' = 1, 2 .$$

Within these conditions the polarization vectors may be chosen differently. Due to the gauge invariance such an uncertainty does not affect physical observables. Indeed, the polarization tensor may be represented as

$$\sum_{\lambda=1,2} \epsilon_\lambda^\mu \epsilon_\lambda^{*\nu} = -g^{\mu\nu} + \text{tensor proportional to } k^\mu \text{ and/or } k^\nu . \quad (3.8)$$

The latter, however, can be dropped since the classical current (3.6c) is explicitly conserving, $(j^\mu k_\mu) = 0$. Therefore one may enjoy the gauge invariance and employ an arbitrary gauge, instead of using the physical polarizations, to calculate accompanying photon production.

The Feynman gauge being the simplest choice, $\sum_{\lambda=1,2} \epsilon_\lambda^\mu \epsilon_\lambda^{*\nu} \implies -g^{\mu\nu}$, we get

$$\begin{aligned} dN &\equiv \frac{dW}{dW_{\text{el}}} = -\frac{\alpha}{4\pi^2} (j^\mu)^2 \omega d\omega d\Omega_\gamma \\ &\simeq \frac{\alpha}{\pi} \frac{d\omega}{\omega} \frac{d\Omega_\gamma}{2\pi} \frac{1 - \cos \Theta_s}{(1 - \cos \Theta_1)(1 - \cos \Theta_2)} . \end{aligned} \quad (3.9)$$

The latter expression corresponds to the relativistic approximation $1 - v_1, 1 - v_2 \ll 1$:

$$-(j^\mu)^2 = \frac{2(p_1 p_2)}{(p_1 k)(p_2 k)} + \mathcal{O}\left(\frac{m^2}{p_0^2}\right) \simeq \frac{2}{\omega^2} \frac{(1 - \vec{n}_1 \cdot \vec{n}_2)}{(1 - \vec{n}_1 \cdot \vec{n})(1 - \vec{n}_2 \cdot \vec{n})} ;$$

it disregards the contribution of *very* small emission angles $\Theta_i^2 \lesssim (1 - v_i^2) = m^2/p_{0i}^2 \ll 1$, where the soft radiation vanishes (the so-called “Dead Cone” region).

If the photon is emitted at a small angle with respect to, say, the incoming particle, i.e. $\Theta_1 \ll \Theta_2 \simeq \Theta_s$, the radiation spectrum (3.9) simplifies to

$$dN \simeq \frac{\alpha}{\pi} \frac{\sin \Theta_1 d\Theta_1}{(1 - \cos \Theta_1)} \frac{d\omega}{\omega} \simeq \frac{\alpha d\Theta_1^2}{\pi \Theta_1^2} \frac{d\omega}{\omega} .$$

Two bremsstrahlung cones appear, centred around incoming and outgoing electron momenta. Inside these cones the radiation has a *double-logarithmic* structure, exhibiting both the *soft* ($d\omega/\omega$) and *collinear* ($d\Theta^2/\Theta^2$) enhancements.

3.2.1. *Low-Barnett-Kroll wisdom*

Soft factorisation (3.6a) is an essence of the celebrated soft bremsstrahlung theorem, formulated by Low in 1956 for the case of scalar charged particles and later generalized by Barnett and Kroll to charged fermions. The very classical nature of soft radiation makes it universal with respect to intrinsic quantum properties of participating objects and the nature of the underlying scattering process: it is only the classical movement of electromagnetic charges that matters.

It is interesting that according to the LBK theorem both the leading $d\omega/\omega$ and the first subleading, $\propto d\omega$, pieces of the soft photon spectrum prove to be “classical”.

For the sake of simplicity we shall leave aside the angular structure of the accompanying photon emission and concentrate on the energy dependence. Then, the relation between the basic cross section $\sigma^{(0)}$ and that with one additional photon with energy ω can be represented symbolically as

$$d\sigma^{(1)}(p_i, \omega) \propto \frac{\alpha d\omega}{\pi \omega} \left[\left(1 - \frac{\omega}{E}\right) \cdot \sigma^{(0)}(p_i) + \left(\frac{\omega}{E}\right)^2 \cdot \tilde{\sigma}(p_i, \omega) \right]. \quad (3.10)$$

The first term in the right-hand side is proportional to the non-radiative cross section $\sigma^{(0)}$. The second term involves the new ω -dependent cross section $\tilde{\sigma}$ which is finite at $\omega = 0$, so that this contribution is suppressed for small photon energies as $(\omega/E)^2$.

This general structure has important consequences, the most serious of which can be formulated, in a dramatic fashion, as

3.2.2. *Soft Photons don't carry quantum numbers*

We are inclined to think that the photon has definite quantum numbers (negative C -parity, in particular). Imagine that the basic process is

forbidden, say, by C -parity conservation. Why not to take off the veto by adding a photon to the system? Surely enough it can be done. There is, however, a price to pay: the selection rules cannot be overcome by *soft* radiation. Since the classical part of the radiative cross section in (3.10) is explicitly proportional to the non-radiative cross section $\sigma^{(0)} = 0$, only *energetic* photons (described by the $\tilde{\sigma}$ term) could do the job. The energy distribution

$$|M|^2 \cdot \frac{d^3k}{\omega} \propto \omega d\omega$$

is typical for a quantum particle, where the production matrix element M is finite in the $\omega \rightarrow 0$ limit, $M = \mathcal{O}(1)$. An enhanced radiation matrix element, $M \propto \omega^{-1}$ characterizes a classical field rather than a quantum object.

So, the price one has to pay to overrule the quantum-number veto by emitting a soft photon with $\omega \ll E$ is the suppression factor $(\omega/E)^2 \ll 1$. We conclude that the photons that are capable of changing the quantum numbers of the system (be it parity, C -parity or angular momentum) cannot be *soft*. Neither can they be *collinear*, by the way, as it follows from the

3.2.3. *Gribov Bremsstrahlung theorem*

This powerful generalisation of the Low theorem states that a simple factorisation holds at the level of the *matrix element*, provided the photon transverse momentum with respect to the radiating charged particle is small compared to the momentum transfers characterising the underlying scattering process:

$$M^{(1)} \propto \frac{(\vec{k}_\perp \cdot \vec{e})}{k_\perp^2} \cdot M^{(0)} + \tilde{M}. \quad (3.11)$$

Here again $\tilde{M} = \text{const}$ in the $k_\perp \rightarrow 0$ limit. This factorisation holds for *hard* photons ($\omega \sim E$) as well as for soft ones.

Both the Low-Barnett-Kroll and the Gribov theorems hold in QCD as well. In particular, it is the Gribov collinear factorisation that leads to the probabilistic evolution picture describing collinear QCD parton multiplication which we shall briefly discuss in the next lecture.

In the QCD context, our statement that “soft photons don’t carry quantum numbers” should be strengthened to even more provocative (but true)

3.2.4. *Soft Gluons don’t carry away no colour*

Don’t rush to protest. Just think it over. In more respectable terms this title can be abbreviated as the NSFL (no-soft-free-lunch) theorem.

Imagine we want to produce a heavy quark $Q\bar{Q}$ bound state (onium) in a hadron-hadron collision. The C -even (χ_Q) mesons can be produced by fusing two quasi-real gluons (with opposite colours) from the QCD parton clouds of the colliding hadrons:

$$(g + g)_{(1)} \rightarrow Q + \bar{Q} \rightarrow \chi_Q. \quad (3.12)$$

In particular, radiative decays of such χ_c mesons are responsible for about 40% of the J/ψ yield. How about the remaining 60%? To directly create a J/ψ (or $\psi' - {}^3S_1$ C -odd $c\bar{c}$ states) two gluons isn't enough. A C -odd meson can decay into, or couple to, *three* photons (like para-positronium does), a photon plus two gluons, or *three* gluons (in a colour-symmetric d_{abc} state).

So, we need one more gluon to attach, for example, in the final state:

$$(g + g)_{(8)} \rightarrow (Q + \bar{Q})_{(8)} \rightarrow J/\psi + g. \quad (3.13)$$

To pick up an initial gg pair in a colour octet state is easier than in the singlet as in (3.12). This, however, does not help to avoid the trouble: the perturbative cross section turns out to be too small to meet the need. It underestimates the Tevatron $p\bar{p}$ data on direct J/ψ and ψ' production by a large factor (up to 50, at large p_\perp).

That very same effect that makes the J/ψ so narrow a meson with the small hadronic decay width $\Gamma_{J/\psi}/M \propto \alpha_s^3(M)$, suppresses its perturbative production cross section (3.13) as well.

Since the perturbative approach apparently fails, it seemed natural to blame the non-perturbative physics. Why not to perturbatively form a colour-octet “ J/ψ ” and then to get rid of colour in a smooth (free of charge) non-perturbative way? To *evaporate* colour does not look problematic: on the one hand, the soft glue distribution is $d\omega/\omega = \mathcal{O}(1)$, on the other hand, the coupling α_s/π in the NP domain may be of the order of unity as well. So why not?

The LBK theorem tells us that either the radiation is soft-enhanced, $\propto d\omega/\omega = \mathcal{O}(1)$, and *classical*, or hard, $\propto \omega d\omega$ and capable of changing the quantum state of the system. Therefore, to rightfully participate in the J/ψ formation as a quantum field, a NP gluon with $\omega \sim \Lambda_{\text{QCD}}$ would have to bring in the suppression factor

$$\left(\frac{\Lambda_{\text{QCD}}}{M_c}\right)^2 \ll 1.$$

The *language* of the LBK is perturbative, 'tis true. The question is, and a serious one indeed, whether the NP phenomena respect the basic dynamical features that its PT counterpart does? Or shall we rather

forget about quantum mechanics, colour conservation, etc. and accept an “anything goes” motto in the NP domain?

To avoid our discussion turning theological, we better address another verifiable issue namely, photoproduction of J/ψ at HERA. Here we have instead of (3.13) the fusion process of a real (photoproduction) or virtual (electroproduction) photon with a quasi-real space-like gluon from the parton cloud of the target proton:

$$\gamma^{(*)} + g \rightarrow (Q + \bar{Q})_{(8)} \rightarrow J/\psi + g. \quad (3.14)$$

If the final-state gluon were soft NP junk, the J/ψ meson would have carried the whole photon momentum and its distribution in Feynman z would peak at $z = 1$ as $(1 - z)^{-1}$. The HERA experiments have found instead a flatish (if not vanishing) z -spectrum at large z . The NSFL theorem seems to be up and running.

By the way, the conventional PT treatment of the photoproduction (3.14) is reportedly doing well. So, what is wrong with the hadroproduction then? Strictly speaking, the problem is still open. An alternative to (3.13) would be to look for the third (hard or *hardish*) gluon in the initial state².

The NSFL QCD discourse has taken us quite far from the mainstream of the introductory lecture. Let us return to the basic properties of QED bremsstrahlung and make a comparative study of

3.3. INDEPENDENT AND COHERENT RADIATION

In the Feynman gauge, the accompanying radiation factor dN in (3.9) is dominated by the *interference* between the two emitters:

$$dN \propto - \left[\frac{p_1^\mu}{(p_1 k)} - \frac{p_2^\mu}{(p_2 k)} \right]^2 \approx \frac{2(p_1 p_2)}{(p_1 k)(p_2 k)}.$$

Therefore it does not provide a satisfactory answer to the question, which part of radiation is due to the initial charge and which is due to the final one?

There is a way, however, to give a reasonable answer to this question. To do that one has to sacrifice simplicity of the Feynman-gauge calculation and recall the original expression (3.7) for the cross section in terms of physical photon polarizations. It is natural to choose the so-called *radiative* (temporal) gauge based on the 3-vector potential \vec{A} , with the

² an interesting, reliable and predictive model for production of onia in the gluon field of colliding hadrons is being developed by Paul Hoyer and collaborators (Hoyer, Marchal & Peigne, 2000)

scalar component set to zero, $A_0 \equiv 0$. Our photon is then described by (real) 3-vectors orthogonal to one another and to its 3-momentum:

$$(\vec{\epsilon}_\lambda \cdot \vec{\epsilon}_{\lambda'}) = \delta_{\lambda\lambda'}, \quad (\vec{\epsilon}_\lambda \cdot \vec{k}) = 0. \quad (3.15)$$

This explicitly leaves us with *two* physical polarization states. Summing over polarizations obviously results in

$$dN \propto \sum_{\lambda=1,2} \left| \vec{j}(k) \cdot \vec{\epsilon}_\lambda \right|^2 = \sum_{\alpha,\beta=1\dots 3} \vec{j}^\alpha(k) \cdot [\delta_{\alpha\beta} - \vec{n}_\alpha \vec{n}_\beta] \cdot \vec{j}^\beta(k), \quad (3.16)$$

with α, β the 3-dimensional indices. We now substitute the soft current (3.6c) in the 3-vector form, $p_i^\mu \rightarrow \vec{v}_i p_{0i}$, and make use of the relations

$$(\vec{v}_i)_\alpha \left[\delta_{\alpha\beta} - \frac{k_\alpha k_\beta}{\vec{k}^2} \right] (\vec{v}_i)_\beta = v_i^2 \sin^2 \Theta_i, \quad (3.17a)$$

$$(\vec{v}_1)_\alpha \left[\delta_{\alpha\beta} - \frac{k_\alpha k_\beta}{\vec{k}^2} \right] (\vec{v}_2)_\beta = v_1 v_2 (\cos \Theta_{12} - \cos \Theta_1 \cos \Theta_2), \quad (3.17b)$$

to finally arrive at

$$dN = \frac{\alpha}{\pi} \{ \mathcal{R}_1 + \mathcal{R}_2 - 2\mathcal{J} \} \cdot \frac{d\omega}{\omega} \frac{d\Omega}{4\pi}. \quad (3.18a)$$

Here

$$\mathcal{R}_i = \frac{v_i^2 \sin^2 \Theta_i}{(1 - v_i \cos \Theta_i)^2}, \quad i = 1, 2, \quad (3.18b)$$

$$\mathcal{J} \equiv \frac{v_1 v_2 (\cos \Theta_{12} - \cos \Theta_1 \cos \Theta_2)}{(1 - v_1 \cos \Theta_1)(1 - v_2 \cos \Theta_2)}. \quad (3.18c)$$

The contributions $\mathcal{R}_{1,2}$ can be looked upon as being due to *independent radiation* off initial and final charges, while the \mathcal{J} -term accounts for *interference* between them. The independent and interference contribution, taken together, describe the *coherent* emission. It is straightforward to verify that (3.18) is identical to the Feynman-gauge result (3.9):

$$\mathcal{R}_{\text{coher.}} \equiv \mathcal{R}_{\text{indep.}} - 2\mathcal{J} = -\omega^2 (j^\mu)^2, \quad \mathcal{R}_{\text{indep.}} \equiv \mathcal{R}_1 + \mathcal{R}_2. \quad (3.19)$$

3.3.1. The rôle of interference: strict angular ordering

In the relativistic limit we have

$$\mathcal{R}_1 \simeq \frac{\sin^2 \Theta_1}{(1 - \cos \Theta_1)^2} = \frac{2}{a_1} - 1, \quad (3.20a)$$

$$\mathcal{J} \simeq \frac{\cos \Theta_{12} - \cos \Theta_1 \cos \Theta_2}{(1 - \cos \Theta_1)(1 - \cos \Theta_2)} = \frac{a_1 + a_2 - a_{12}}{a_1 a_2} - 1 \quad (3.20b)$$

where we introduced a convenient notation

$$\begin{aligned} a_1 &= 1 - \vec{n}\vec{n}_1 = 1 - \cos \Theta_1, & a_2 &= 1 - \cos \Theta_2, \\ a_{12} &= 1 - \vec{n}_1\vec{n}_2 = 1 - \cos \Theta_s. \end{aligned}$$

The variables a are small when the angles are small: $a \simeq \frac{1}{2}\Theta^2$.

The independent radiation has a typical logarithmic behaviour up to large angles:

$$dN_1 \propto \mathcal{R}_1 \sin \Theta d\Theta \propto \frac{da_1}{a_1}, \quad a_1 \lesssim 1.$$

However, the interference effectively cuts off the radiation at angles exceeding the scattering angle:

$$dN \propto \mathcal{R}_{\text{coher.}} \sin \Theta d\Theta = 2a_{12} \frac{da}{a_1 a_2} \propto \frac{da}{a^2} \propto \frac{d\Theta^2}{\Theta^4}, \quad a \equiv a_1 \simeq a_2 \gg a_{12}.$$

To quantify this coherent effect, let us combine an independent contribution with a half of the interference one to define

$$V_1 = \mathcal{R}_1 - \mathcal{J} = \frac{2}{a_1} - \frac{a_1 + a_2 - a_{12}}{a_1 a_2} = \frac{a_{12} + a_2 - a_1}{a_1 a_2}, \quad (3.21a)$$

$$V_2 = \mathcal{R}_2 - \mathcal{J} = \frac{2}{a_2} - \frac{a_1 + a_2 - a_{12}}{a_1 a_2} = \frac{a_{12} + a_1 - a_2}{a_1 a_2};$$

$$\mathcal{R}_{\text{coher.}} = V_1 + V_2. \quad (3.21b)$$

The emission probability V_i can be still considered as “belonging” to the charge $\#i$ (V_1 is singular when $a_1 \rightarrow 0$, and vice versa). At the same time these are no longer *independent* probabilities, since V_1 explicitly depends on the direction of the partner-charge $\#2$; *conditional* probabilities, so to say.

It is straightforward to verify the following remarkable property of the “conditional” distributions V : after *averaging* over the *azimuthal angle* of the radiated quantum, \vec{n} , with respect to the direction of the parent charge, \vec{n}_1 , the probability $V_1(\vec{n}, \vec{n}_1; \vec{n}_2)$ *vanishes* outside the Θ_s -cone. Namely

$$\langle V_1 \rangle_{\text{azimuth}} \equiv \int_0^{2\pi} \frac{d\phi_{n,n_1}}{2\pi} V_1(\vec{n}, \vec{n}_1; \vec{n}_2) = \frac{2}{a_1} \vartheta(a_{12} - a_1). \quad (3.22)$$

It is only a_2 that changes under the integral (3.22), while a_1 , and obviously a_{12} , stay fixed. The result follows from the angular integral

$$\int_0^{2\pi} \frac{d\phi_{n,n_1}}{2\pi} \frac{1}{a_2} = \frac{1}{|\cos \Theta_1 - \cos \Theta_s|} = \frac{1}{|a_{12} - a_1|}.$$

Naturally, a similar expression for V_2 emerges after the averaging over the azimuth around \vec{n}_2 is performed.

We conclude that as long as the *total* (angular-integrated) emission probability is concerned, the result can be expressed as a sum of two independent bremsstrahlung cones centred around \vec{n}_1 and \vec{n}_2 , both having the finite opening half-angle Θ_s .

This nice property is known as a “strict angular ordering”. It is an essential part of the so-called Modified Leading Log Approximation (MLLA), which describes the internal structure of parton jets with a single-logarithmic accuracy.

3.3.2. *Angular ordering on the back of envelope*

What is the reason for radiation at angles exceeding the scattering angle to be suppressed? Let us try our physical intuition and consider semi-classically how the radiation process really develops.

A physical electron is a charge surrounded by its proper Coulomb field. In quantum language the Lorentz-contracted Coulomb-disk attached to a relativistic particle may be treated as consisting of photons virtually emitted and, in due time, re-absorbed by the core charge. Such virtual emission and absorption processes form a coherent state which we call a physical electron (“dressed” particle).

This coherence is partially destroyed when the charge experiences an impact. As a result, a part of intrinsic field fluctuations gets released in the form of real photon radiation: the bremsstrahlung cone in the direction of the initial momentum develops. On the other hand, the deflected charge now leaves the interaction region as a “half-dressed” object with its proper field-coat lacking some field components (eventually those that were lost at the first stage). In the process of regenerating the new Coulomb-disk adjusted to the final-momentum direction, an extra radiation takes place giving rise to the second bremsstrahlung cone.

Now we need to be more specific to find out which momentum components of the electromagnetic coat do actually take leave.

A typical time interval between emission and re-absorption of the photon k by the initial electron p_1 may be estimated as the Lorentz-dilated lifetime of the virtual intermediate electron state $(p_1 - k)$ (see the left graph in Fig. 7,

$$t_{\text{fluct}} \sim \frac{E_1}{|m^2 - (p_1 - k)^2|} = \frac{E_1}{2p_1 k} \sim \frac{1}{\omega \Theta^2} = \frac{\omega}{k_{\perp}^2}. \quad (3.23)$$

Here we restricted ourselves, for simplicity, to small radiation angles, $k_{\perp} \approx \omega \Theta \ll k_{\parallel} \approx \omega$. The fluctuation time (3.23) may become macroscopically large for small photon energies ω and enters as a characteristic parameter in a number of QED processes. As an example, let us men-

tion the so called Landau-Pomeranchuk effect — suppression of soft radiation off a charge that experiences multiple scattering propagating through a medium. Quanta with too large a wavelength get not enough time to be properly formed before successive scattering occurs, so that the resulting bremsstrahlung spectrum behaves as $dN \propto d\omega/\sqrt{\omega}$ instead of the standard logarithmic $d\omega/\omega$ distribution.

The characteristic time scale (3.23) responsible for this and many other radiative phenomena is often referred to as the *formation time*.

Now imagine that within this interval the core charge was kicked by some external interaction and has changed direction by some Θ_s . Whether the photon will be re-absorbed or not depends on the position of the scattered charge with respect to the point where the photon was expecting to meet it “at the end of the day”. That is, we need to compare the spatial displacement of the core charge $\Delta\vec{r}$ with the characteristic size of the photon field, $\lambda_{\parallel} \sim \omega^{-1}$, $\lambda_{\perp} \sim k_{\perp}^{-1}$:

$$\begin{aligned}\Delta r_{\parallel} &\sim \left| v_{2\parallel} - v_{1\parallel} \right| \cdot t_{\text{fluct}} \sim \Theta_s^2 \cdot \frac{1}{\omega\Theta^2} = \left(\frac{\Theta_s}{\Theta} \right)^2 \lambda_{\parallel} \Leftrightarrow \lambda_{\parallel}; \\ \Delta r_{\perp} &\sim c\Theta_s \cdot t_{\text{fluct}} \sim \Theta_s \cdot \frac{1}{\omega\Theta^2} = \left(\frac{\Theta_s}{\Theta} \right) \lambda_{\perp} \Leftrightarrow \lambda_{\perp}.\end{aligned}\tag{3.24}$$

For large scattering angles, $\Theta_s \sim 1$, the charge displacement exceeds the photon wavelength for arbitrary Θ , so that the two full-size bremsstrahlung cones are present. For numerically small $\Theta_s \ll 1$, however, it is only photons with $\Theta \lesssim \Theta_s$ that can notice the charge being displaced and thus the coherence of the state being disturbed. Therefore only the radiation at angles smaller than the scattering angle actually emerges. The other field components have too large a wavelength and are easily re-absorbed *as if* there were no scattering at all.

So what counts is a change in the current, which is sharp enough to be noticed by the “to-be-emitted” quantum within the characteristic formation/field-fluctuation time (3.23) of the latter.

Radiation at large angles has too short a formation time to become aware of the acceleration of the charge. No scattering — no radiation.

The same argument applies to the dual process of production of two opposite charges (decay of a neutral object, vacuum pair production, etc.). The only difference is that now one has to take for $\Delta\vec{r}$ not a displacement between the initial and the final charges, but the actual distance between the produced particles (spatial size of a dipole), to be compared with the radiation wavelength.

3.4. QCD SCATTERING AND CROSS-CHANNEL RADIATION

Both the qualitative arguments of the previous sections and the quantitative analysis of the two-particle antenna pattern apply to the QCD process of gluon emission in the course of quark scattering. So two gluon-bremsstrahlung cones with the opening angles restricted by the scattering angle Θ_s would be expected to appear.

There is an important subtlety, however. In the QED case it was deflection of an electron that changed the e.m. current and caused photon radiation. In QCD there is another option, namely to “repaint” the quark. Rotation of the *colour state* would affect the colour current as well and, therefore, must lead to gluon radiation irrespectively of whether the quark-momentum direction has changed or not.

This is what happens when a quark scatters off a *colour* field. To be specific, one may consider as an example two channels of Higgs production in hadron-hadron collisions.

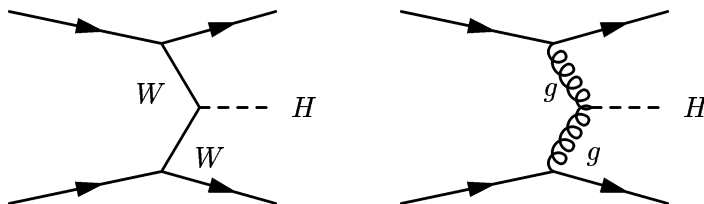


Figure 8. WW and gluon-gluon fusion graphs for Higgs production

At very high energies two mechanisms of Higgs production become competitive: $W^+W^- \rightarrow H$ and the gluon-gluon fusion $gg \rightarrow H$ (see Fig. 8).

Since the typical momentum transfer is large, of the order of the Higgs mass, $(-t) \sim M_H^2$, Higgs production is a *hard* process. Colliding quarks experience hard scattering with characteristic scattering angles $\Theta_s^2 \simeq |t|/s \sim M_H^2/s$. As far as the accompanying gluon radiation is concerned, the two subprocesses differ with respect to the nature of the “external field”, which is *colorless* for the W -exchange and *colorful* for the gluon fusion.

The gluon bremsstrahlung amplitudes for the second case are shown in Fig. 9. In principle, a graph with the gluon-gluon interaction vertex should also be considered. However, in the limit $k_\perp \ll q_\perp$, with $\vec{q}_\perp \approx \vec{p}_{2\perp} - \vec{p}_{1\perp}$ the momentum transfer in the scattering process, emission off the external lines dominates (the “soft insertion rules”).

The accompanying soft radiation current j^μ factors out from the Feynman amplitudes of Fig. 9, the only difference with the Abelian

current (3.6c) being the order of the colour generators:

$$j^\mu = \left[t^b t^a \left(\frac{p_1^\mu}{(p_1 k)} \right) - t^a t^b \left(\frac{p_2^\mu}{(p_2 k)} \right) \right]. \quad (3.25)$$

Introducing the abbreviation $A_i = \frac{p_i^\mu}{(p_i k)}$, we apply the standard decomposition of the product of two triplet colour generators,

$$t^a t^b = \frac{1}{2N_c} \delta_{ab} + \frac{1}{2} (d_{abc} + i f_{abc}) t^c,$$

to rewrite (3.25) as

$$j^\mu = \frac{1}{2} (A_1 - A_2) \left(\frac{1}{N} \delta^{ab} + d^{abc} t^c \right) - \frac{1}{2} (A_1 + A_2) i f^{abc} t^c.$$

To find the emission *probability* we need to construct the product of the currents and sum over colours. Three colour structures do not “interfere”, so it suffices to evaluate the squares of the singlet, $\mathbf{8}_s$ and $\mathbf{8}_a$ structures:

$$\begin{aligned} \sum_{a,b} \left(\frac{1}{2N_c} \delta_{ab} \right)^2 &= \left(\frac{1}{2N} \right)^2 (N_c^2 - 1) = \frac{1}{2N_c} \cdot C_F; \\ \sum_{a,b} \left(\frac{1}{2} d_{abc} t^c \right)^2 &= \frac{1}{4} \frac{N_c^2 - 4}{N_c} (t^c)^2 = \frac{N_c^2 - 4}{4N_c} \cdot C_F; \\ \sum_{a,b} \left(\frac{1}{2} i f_{abc} t^c \right)^2 &= \frac{1}{4} N_c (t^c)^2 = \frac{N_c}{4} \cdot C_F. \end{aligned}$$

The common factor $C_F = (t^b)^2$ belongs to the Born (non-radiative) cross section, so that the radiation spectrum takes the form

$$\begin{aligned} dN \propto \frac{1}{C_F} \sum_{\text{colour}} j^\mu \cdot (j_\mu)^* &= \left(\frac{1}{2N_c} + \frac{N_c^2 - 4}{4N_c} \right) (A_1 - A_2) \cdot (A_1 - A_2) \\ &+ \frac{N_c}{4} (A_1 + A_2) \cdot (A_1 + A_2). \end{aligned}$$

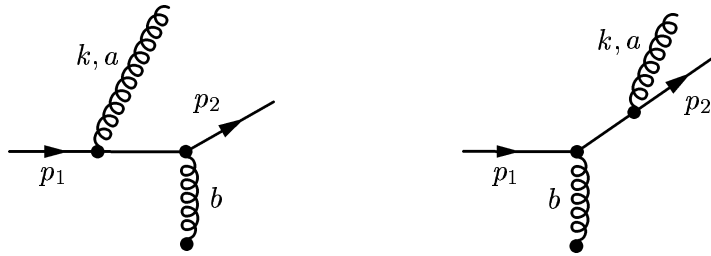


Figure 9. Gluonic Bremsstrahlung diagrams for $k_\perp \ll q_\perp$. The characters a and b denote the colours of the radiated and exchanged gluons.

A simple algebra leads to

$$dN \propto C_F (A_1 - A_2) \cdot (A_1 - A_2) + N_c A_1 \cdot A_2. \quad (3.26)$$

Dots here symbolize the sum over gluon polarization states. To calculate the cross section some care should be exercised: the current (3.25) *does not conserve* because of non-commuting colour matrices. We would need to include gluon radiation from the exchange-gluon line *and* from the source, to be in a position to use an arbitrary gauge (e.g. the Feynman gauge) for the emitted gluon. The physical polarization technique (3.15) simplifies our task. To obtain the true accompanying radiation pattern (in the $k_\perp \ll q_\perp$ region) it suffices to use the projectors (3.17) for the dots in (3.26). In particular,

$$A_1 \cdot A_2 \equiv \sum_{\lambda=1,2} \left(A_1 e^{(\lambda)} \right) \left(A_2 e^{(\lambda)} \right)^* = \mathcal{J} \quad \{ \neq -(A_1 A_2) \text{ sic!} \}.$$

Accompanying radiation intensity finally takes the form

$$dN \propto C_F \mathcal{R}_{\text{coher.}} + N_c \mathcal{J}. \quad (3.27)$$

The first term proportional to the squared quark charge is responsible, as we already know, for two narrow bremsstrahlung cones around the incoming and outgoing quarks, $\Theta_1, \Theta_2 \leq \Theta_s$. On top of that an additional, purely non-Abelian, contribution shows up, which is proportional to the *gluon* charge. It is given by the interference distribution (3.18c), (3.20b),

$$\mathcal{J} = \frac{a_1 + a_2 - a_{12}}{a_1 a_2} - 1,$$

which remains *non-singular* in the forward regions $\Theta_1 \ll \Theta_s$ and $\Theta_2 \ll \Theta_s$. At the same time, it populates large emission angles $\Theta = \Theta_1 \approx \Theta_2 \gg \Theta_s$ where

$$dN \propto d\Omega \mathcal{J} \propto \sin \Theta d\Theta \left(\frac{2}{a} - 1 \right) \sim \frac{d\Theta^2}{\Theta^2}. \quad (3.28)$$

Indeed, evaluating the azimuthal average, say, around the *incoming* quark direction we obtain

$$\int \frac{d\phi_1}{2\pi} \mathcal{J} = \frac{1}{a_1} \left(1 + \frac{a_1 - a_{12}}{|a_1 - a_{12}|} \right) - 1 = \frac{2}{a_1} \vartheta(\Theta_1 - \Theta_s) - 1.$$

Thus we conclude that the third complementary bremsstrahlung cone emerges. It basically corresponds to radiation at angles *larger* than the scattering angle and its intensity is proportional to the colour charge of the *t*-channel exchange.

We could have guessed without actually performing the calculation that at large angles the gluon radiation is related to the *gluon* colour charge. As far as large emission angles $\Theta \gg \Theta_s$ are concerned, one may identify the directions of initial and final particles to simplify the total radiation amplitude as

$$j^\mu = T^b T^a \cdot \frac{p_1^\mu}{p_1 k} - T^a T^b \cdot \frac{p_2^\mu}{p_2 k} \approx (T^b T^a - T^a T^b) \cdot \frac{p^\mu}{pk}.$$

Recalling the general commutation relation for the $SU(N_c)$ generators,

$$[T^a(R), T^b(R)] = i \sum_c f_{abc} T^c(R), \quad (3.29)$$

we immediately obtain the factor $N_c \propto (if_{abc})^2$ as the proper colour charge. Since (3.29) holds for arbitrary colour representation R , we see that the accompanying gluon radiation at large angles $\Theta > \Theta_s$ does not depend on the nature of the projectile.

The bremsstrahlung gluons we are discussing transform, in the end of the day, into observable final hadrons. We are ready now to derive an interesting physical prediction from our QCD soft radiation exercise.

Translating the emission angle into (pseudo)rapidity $\eta = \ln \Theta^{-1}$, the logarithmic angular distribution (3.28) converts into the rapidity plateau. We conclude that in the case of the gluon fusion mechanism, the second in Fig. 8, the hadronic accompaniment should form a practically uniform rapidity plateau. Indeed, the hadron density in the centre (small η , large c.m.s. angles) is proportional to the gluon colour charge N_c , while in the “fragmentation regions” ($\eta_{\max} > |\eta| > \ln \Theta_s^{-1}$, or $\Theta < \Theta_s$) the two quark-generated bremsstrahlung cones give, roughly speaking, the density $\sim 2 \times C_F \approx N_c$.

At the same time, the WW -fusion events (the first graph in Fig. 8) should have an essentially different final state structure. Here we have a colorless exchange, and the QED-type angular ordering, $\Theta < \Theta_s$, restricts the hadronic accompaniment to the two projectile fragmentation humps as broad as $\Delta\eta = \eta_{\max} - \ln \Theta_s \simeq \ln M_H$, while the central rapidity region should be devoid of hadrons. The “rapidity gap” is expected which spans over $|\eta| < \ln(\sqrt{s}/M_H)$.

3.5. CONSERVATION OF COLOUR CURRENT

In physical terms universality of the generator algebra is intimately related with *conservation of colour*. To illustrate this point let us consider production of a quark-gluon pair in some hard process and address the question of how this system radiates. Let p and k be the momenta of the quark and the gluon, with b the octet colour index of the latter. For the

sake of simplicity we concentrate on *soft* accompanying radiation, which determines the bulk of particle multiplicity inside jets, the structure of the hadronic plateau, etc. As far as emission of a soft gluon with momentum $\ell \ll k, p$ is concerned, the so-called “soft insertion rules” apply, which tell us that the Feynman diagrams dominate where ℓ is radiated off the external (real) partons — the final quark line p and the gluon k . The corresponding Feynman amplitudes are shown in Fig. 10.

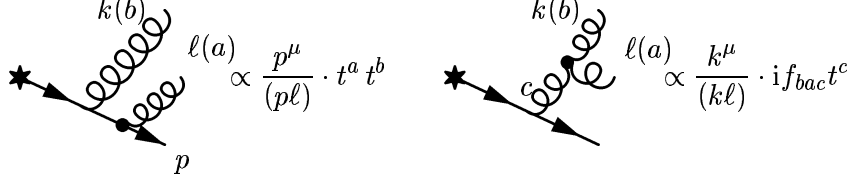


Figure 10. Feynman diagrams for radiation of the soft gluon with momentum ℓ and colour a off the qg system.

Do two emission amplitudes interfere with each other? It depends on the direction of the radiated gluon $\vec{\ell}$.

In the first place, there are two bremsstrahlung cones centred around the directions of \vec{p} and \vec{k} :

$$\begin{aligned} \text{quark cone: } \Theta_{\vec{\ell}} &\equiv \Theta_{\vec{\ell}, \vec{p}} \ll \Theta \approx \Theta_{\vec{\ell}, \vec{k}}, \\ \text{gluon cone: } \Theta_{\vec{\ell}} &\equiv \Theta_{\vec{\ell}, \vec{k}} \ll \Theta \approx \Theta_{\vec{\ell}, \vec{p}}, \end{aligned}$$

with Θ the angle between \vec{p} and \vec{k} — the aperture of the qg fork. In these regions one of the two amplitudes of Fig. 10 is much larger than the other, and the interference is negligible: the gluon ℓ is radiated independently and participates in the formation of the quark and gluon sub-jets.

If Θ is sufficiently large and the gluon k sufficiently energetic (relatively hard, $k \sim p$), these two sub-jets can be distinguished in the final state. The particle density in q and g jets should be remarkably different. It should be proportional (at least asymptotically) to the probability of soft gluon radiation which, in turn, is proportional to the “squared colour charge” of a the jet-generating parton, quark or gluon:

$$\left(\ell \frac{dn}{d\ell} \right)_{\Theta_{\vec{\ell}} < \Theta}^g : \left(\ell \frac{dn}{d\ell} \right)_{\Theta_{\vec{\ell}} < \Theta}^q = N_c : \frac{N_c^2 - 1}{2N_c} = 3 : \frac{4}{3} = \frac{9}{4}.$$

Multi-jet configurations are comparatively rare: emission of an additional hard gluon $k \sim p$ at large angles $\Theta \sim 1$ constitutes a fraction $\alpha_s/\pi \lesssim 10\%$ of all events. Typically k would prefer to belong to the

quark bremsstrahlung cone itself, that is to have $\Theta \ll 1$. In such circumstances the question arises about the structure of the accompanying radiation at comparatively *large* angles

$$\Theta_{\vec{\ell}} \equiv \Theta_{\vec{\ell}, \vec{p}} \simeq \Theta_{\vec{\ell}, \vec{k}} \gg \Theta. \quad (30)$$

If the quark and the gluon were acting as independent emitters, we would expect the particle density to increase correspondingly and to overshoot the standard quark jet density by the factor

$$\left(\ell \frac{dn}{d\ell} \right)_{\Theta_{\vec{\ell}} > \Theta}^{g+q} : \left(\ell \frac{dn}{d\ell} \right)_{\Theta_{\vec{\ell}} > \Theta}^q = N_c : \frac{N_c^2 - 1}{2N_c} + 1 = \frac{13}{4}. \quad (31)$$

However, in this angular region our amplitudes start to interfere significantly, so that the radiation off the qg pair is no longer given by the *sum of probabilities* $q \rightarrow g(\ell)$ plus $g \rightarrow g(\ell)$. We have to square the *sum of amplitudes* instead.

This can be easily done by observing that in the large-angle kinematics (30) the angle Θ between \vec{p} and \vec{k} can be neglected, so that the accompanying soft radiation factors in Fig. 10 become indistinguishable,

$$\frac{p^\mu}{(p\ell)} \simeq \frac{k^\mu}{(k\ell)}.$$

Thus the Lorentz structure of the amplitudes becomes the same and it suffices to sum the colour factors:

$$t^a t^b + if_{bac} t^c = t^a t^b + [t^b, t^a] \equiv t^b t^a. \quad (32)$$

We conclude that the coherent sum of two amplitudes of Fig. 10 results in radiation at large angles *as if* off the initial quark, as shown in Fig. 11.

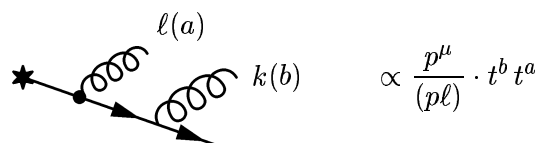


Figure 11. Soft radiation at large angles is determined by the total colour charge

This means that the naive probabilistic expectation of enhanced density (31) fails and the particle yield is equal to that for the quark-initiated jet instead: $13/4 \rightarrow 1$.

It actually does not matter whether the gluon k was present at all, or whether there was instead a whole bunch of partons with small

relative angles between them. Soft gluon radiation at large angles is sensitive only to the *total* colour charge of the final parton system, which equals the colour charge of the initial parton. This physically transparent statement holds not only for the quark as in Figs. 10, 11 but for an arbitrary object R (gluon, diquark, . . . , you name it) as an initial object. In this case the matrices $t = T(3)$ should be replaced by the generators $T(R)$ corresponding to the colour representation R , and (32) holds due to the universality of the generator algebra (3.29).

4. Coherence in QCD parton cascades

Allowing small relative angles between partons in a process with a large hardness Q^2 results in a logarithmic enhancement of the emission probability:

$$\alpha_s \implies \alpha_s \frac{d\Theta^2}{\Theta^2} \rightarrow \alpha_s \log Q^2. \quad (4.33a)$$

As a result, the total probability of one parton (E) turning into two ($E_1 \sim E_2 \sim \frac{1}{2}E$) may become of order 1, in spite of the smallness of the characteristic coupling, $\alpha_s(Q^2) \propto 1/\log Q^2$. A typical example of such a “collinear” enhancement — the splitting process $g \rightarrow q\bar{q}$.

Moreover, when we consider the *gluon* offspring, another — “soft” — enhancement enters the game, which is due to the fact that the gluon bremsstrahlung tends to populate the region of *relatively* small energies ($E \simeq E_1 \gg E_2 \equiv \omega$):

$$\alpha_s \implies \alpha_s \frac{d\omega}{\omega} \frac{d\Theta^2}{\Theta^2} \rightarrow \alpha_s \log^2 Q^2. \quad (4.33b)$$

Thus the true perturbative “expansion parameter” responsible for parton multiplication via $q \rightarrow qg$ and $g \rightarrow gg$ may actually become *much larger* than 1!

In such circumstances we cannot trust the perturbative expansion in $\alpha_s \ll 1$ unless the logarithmically enhanced contributions (4.33) are taken full care of in all orders.

Fortunately, in spite of the complexity of high order Feynman diagrams, such a programme can be carried out. The very fact that the all-order logarithmic asymptotes can be written down in a closed form and, more than that, that they *a posteriori* prove to be quite simple, follows from the **classical nature** of

- *soft* enhancement of bremsstrahlung amplitudes (“infrared” singularities) and

- *collinear* enhancement of basic $1 \rightarrow 2$ parton splitting amplitudes (or “mass” singularities).

As a result, the leading logarithmic asymptotes can be found without performing laborious calculations. It suffices to invoke an intuitively clear picture of parton cascades described in probabilistic fashion in terms of sequential independent elementary parton branchings *ordered in fluctuation times*.

4.1. PUZZLE OF DIS AND PARTONS

Let us invoke the deep inelastic lepton-hadron scattering — a classical example of a hard process and the standard QCD laboratory for carrying out the PT-resummation programme.

Here, the momentum q with a large space-like virtuality $Q^2 = |q^2|$ is transferred from an incident electron (muon, neutrino) to the target proton, which then breaks up into the final multi-parton \rightarrow multi-hadron system. Introducing an invariant energy s between the exchange photon (Z^0, W^\pm) and the proton with 4-momentum P ($P^2 = M_p^2$), one writes the invariant mass of the produced hadron system which measures *inelasticity* of the process as

$$W^2 \equiv (q+P)^2 - M_p^2 = q^2 + 2(Pq) = s(1-x), \quad s = 2(Pq), \quad x \equiv \frac{Q^2}{2(Pq)} \leq 1,$$

with x the Bjorken variable. The cross section of the process depends on two variables: Q^2 and x . For the case of *elastic* lepton-proton scattering one has $x=1$ and it is natural to write the cross section as

$$\frac{d\sigma_{el}}{dQ^2 [dx]} = \frac{d\sigma_{Ruth}}{dQ^2} \cdot f_{el}^2(Q^2) \cdot [\delta(1-x)]. \quad (4.34a)$$

Here $\sigma_{Ruth} \propto \alpha^2/Q^4$ is the standard Rutherford cross section for e.m. scattering off a point charge and f_{el} stands for the elastic proton form factor.

For inclusive *inelastic* cross section one can write an analogous expression by introducing an inelastic proton “form factor” which now depends on both the momentum transfer Q^2 and the inelasticity parameter x :

$$\frac{d\sigma_{in}}{dQ^2 dx} = \frac{d\sigma_{Ruth}}{dQ^2} \cdot f_{in}^2(x, Q^2). \quad (4.34b)$$

What kind of Q^2 -behaviour of the form factors (4.34) could one expect in the Bjorken limit $Q^2 \rightarrow \infty$? Quantum mechanics tells us how the

Q^2 -behaviour of the electromagnetic form factor can be related to the charge distribution inside a proton:

$$f_{el}(Q^2) = \int d^3r \rho(\vec{r}) \exp \{i\vec{Q}\vec{r}\}. \quad (4.35)$$

For a point charge $\rho(\vec{r}) = \delta^3(\vec{r})$, it is obvious that $f \equiv 1$. On the contrary, for a smooth charge distribution $f(Q^2)$ falls with increasing Q^2 , the faster the smoother ρ is. Experimentally, the elastic $e-p$ cross section does decrease with Q^2 *much faster* than the Rutherford one ($f_{el}(Q^2)$ decays as a large power of Q^2). Does this imply that $\rho(\vec{r})$ is indeed regular so that there is no well-localized — point-charge inside a proton? If it were the case, the *inelastic* form factor would decay as well in the Bjorken limit: a tiny photon with the characteristic size $\sim 1/Q \rightarrow 0$ would penetrate through a “smooth” proton like a knife through butter, inducing neither elastic nor inelastic interactions.

However, as was first observed at SLAC in the late sixties, for a fixed x , f_{in}^2 stays practically constant with Q^2 , that is, the inelastic cross section (with a given inelasticity) is similar to the Rutherford cross section (Bjorken scaling). It looks *as if* there was a point-like scattering in the guts of it, but in a rather strange way: it results in inelastic breakup dominating over the elastic channel. Quite a paradoxical picture emerged; Feynman-Bjorken partons came to the rescue.

Imagine that it is not the proton itself that is a point-charge-bearer, but some other guys (quark-partons) inside it. If those constituents were *tightly* bound to each other, the elastic channel would be bigger than, or comparable with, the inelastic one: an excitation of the parton that takes an impact would be transferred, with the help of rigid links between partons, to the proton as a whole, leading to the elastic scattering or to the formation of a quasi-elastic finite-mass system ($N\pi$, $\Delta\pi$ or so), $1-x \ll 1$.

To match the experimental pattern $f_{el}^2(Q^2) \ll f_{in}^2(Q^2)$ one has instead to view the parton ensemble as a *loosely* bound system of quasi-free particles. Only under these circumstances does knocking off one of the partons inevitably lead to deep inelastic breakup, with a negligible chance of reshuffling the excitation among partons.

The parton model, forged to explain the DIS phenomenon, was intrinsically paradoxical by itself. In sixties and seventies, there was no other way of discussing particle interactions but in the field-theoretical framework, where it remains nowadays. But all reliable (renormalisable, 4-dimensional) quantum field theories (QFTs) known by then had one feature in common: an effective interaction strength (the running coupling $g^2(Q^2)$) *increasing* with the scale of the hard process Q^2 . Actually, this feature was widely believed to be a general law of nature, and for

a good reason³. At the same time, it would be preferable to have it the other way around so as to be in accord with the parton model, which needs parton-parton interaction to *weaken* at small distances (large Q^2).

Only with the advent of non-Abelian QFTs (and QCD among them) exhibiting an anti-intuitive asymptotic-freedom behaviour of the coupling, the concept of partons was to become more than a mere phenomenological model.

4.2. QCD PARTON PICTURE

Typical QCD graphs for DIS amplitudes are shown in Fig. 12.

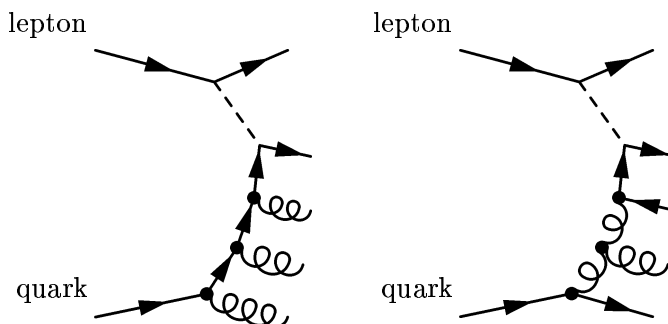


Figure 12. Valence (left) and Bethe-Heitler mechanism (right) of DIS.

For moderate x -values (say, $x > 0.1$) the process is dominated by lepton scattering off a valence quark in the proton. The scattering cross section has a standard energy behaviour $\sigma \propto x^{-2(J_{\text{ex}}-1)}$, where J_{ex} is the spin of the exchanged particle in the t -channel. It is the quark with $J_{\text{ex}} = \frac{1}{2}$ in the left picture of Fig. 12, so that the valence contribution to the cross section decreases at small x as $\sigma \propto x$.

For high-energy scattering, $x \ll 1$, the Bethe-Heitler mechanism takes over which corresponds to the t -channel *gluon* exchange: $J_{\text{ex}} = 1$, $\sigma \propto x^0 = \text{const}$ (modulo logarithms).

In the Leading Logarithmic Approximation (LLA) one insists on picking up, for each new parton taken into consideration, a logarithmic enhancement factor $\alpha_s \rightarrow \alpha_s \log Q^2$. In this approximation the scattering *probability* can be simply obtained by convoluting elementary probabilities of independent $1 \rightarrow 2$ parton splittings.

³ relation between screening and unitarity

To cut a long story short, the appearance of the log-enhanced contributions in (4.33a) is due to the following structure

$$\begin{aligned} \frac{1}{n!} \left[\frac{\alpha_s}{\pi} \ln \frac{Q^2}{\mu^2} \right]^n &= \left[\frac{\alpha_s}{\pi} \right]^n \int^{Q^2} \frac{dk_{\perp n}^2}{k_{\perp n}^2} \int^{k_{\perp n}^2} \frac{dk_{\perp n-1}^2}{k_{\perp n-1}^2} \dots \\ &\dots \int^{k_{\perp 3}^2} \frac{dk_{\perp 2}^2}{k_{\perp 2}^2} \int_{\mu^2}^{k_{\perp 2}^2} \frac{dk_{\perp 1}^2}{k_{\perp 1}^2}, \end{aligned} \quad (4.36)$$

with $k_{\perp i}^2$ the squared transverse momenta of produced partons.

To contribute to the LLA, the transverse momenta of produced partons should be strongly ordered, increasing up the ‘‘ladder’’: $k_{\perp 1}^2 \ll \dots \ll k_{\perp n}^2 \ll Q^2$. (At the level of Feynman *amplitudes* the ladder diagrams dominate, provided a special physical gauge is chosen for gluon fields.) This expression diverges in the zero-quark-mass limit, $\mu \rightarrow 0$. Well, when you see a nasty thing happen beyond your reach, you can do no better than make use of it. This ‘‘mass singularity’’, according to (4.36), occurs in the lower limit of the k_{\perp} integration of the very first (and only!) parton branch. Let us drag this misbehaving integral to the left by rewriting (4.36) as

$$\begin{aligned} (4.36)^{[n]}(Q^2, \mu^2) &= \frac{\alpha_s}{\pi} \int_{\mu^2}^{Q^2} \frac{dk_{\perp 1}^2}{k_{\perp 1}^2} \left[\frac{\alpha_s}{\pi} \right]^{n-1} \int^{Q^2} \frac{dk_{\perp n}^2}{k_{\perp n}^2} \int^{k_{\perp n}^2} \frac{dk_{\perp n-1}^2}{k_{\perp n-1}^2} \dots \\ &\dots \int_{k_{\perp 1}^2}^{k_{\perp 3}^2} \frac{dk_{\perp 2}^2}{k_{\perp 2}^2} = \frac{\alpha_s}{\pi} \int_{\mu^2}^{Q^2} \frac{dk_{\perp 1}^2}{k_{\perp 1}^2} (4.36)^{[n-1]}(Q^2, k_{\perp 1}^2), \end{aligned}$$

where we have combined the internal $(n-1)$ integrals into the same expression that corresponds to the previous order in α_s -expansion and has a new lower limit $k_{\perp 1}^2$ substituted for the original μ^2 . Now, we can localize the μ -dependence by evaluating the logarithmic derivative:

$$\mu^2 \frac{\partial}{\partial \mu^2} (4.36)^{[n]} = -\frac{\alpha_s}{\pi} \cdot (4.36)^{[n-1]}.$$

This equation relates the n^{th} order of the PT expansion to the previous one. To put this symbolic relation at work one first has to recall the satellite x -dependence.

By extracting the first step one may look upon the rest as DIS off a new ‘‘target’’ — the parton with transverse momentum $k_{\perp 1}^2$ and a finite fraction z of the initial longitudinal momentum P . As a result, there appears an additional integration with the probability of the first splitting, $\phi(z)$, and the differential equation for the resummed $F^{\text{(LLA)}}$ takes the form

$$\mu^2 \frac{\partial}{\partial \mu^2} F(x, Q^2, \mu^2) = -\int_x^1 \frac{dz}{z} \phi(z) \frac{\alpha_s}{\pi} \cdot F\left(\frac{x}{z}, Q^2, \mu^2\right). \quad (4.37a)$$

Since a logarithm (like a stick) has two ends, differentiation over the overall hardness scale Q^2 would do the same job, the result being the *evolution equation* in a familiar form:

$$Q^2 \frac{\partial}{\partial Q^2} F(x, Q^2) = \frac{\alpha_s}{\pi} \phi(x) \otimes F(x, Q^2), \quad (4.37b)$$

where the symbol \otimes stands for convolution in the x -space.

4.3. LLA PARTON EVOLUTION

4.3.1. Apparent and hidden symmetries of the QCD evolution

Since (4.37b) reminds of a Schrödinger (diffusion) equation (with $dt = \frac{\alpha_s}{\pi} dQ^2/Q^2$ as the “evolution time” differential), we can refer to the kernels $\phi(x)$ as the matrix elements of the “evolution Hamiltonian” in the (F, G) space, where F marks a spin- $\frac{1}{2}$ quark (fermion) and G a vector gluon.

To discuss the relations between kernels it is convenient to extract colour factors

$$\begin{aligned} t_{ij}^a t_{jk}^a &= C_F \delta_{ik}, & t_{ik}^a t_{ki}^b &= T_R \delta^{ab} = \frac{1}{2} \delta^{ab}, & f_{ade} f_{bde} &= N_c \delta_{ab}; \\ \Phi_F^F(z) &= C_F \cdot V_F^F(z) & \Phi_F^G(z) &= C_F \cdot V_F^G(z), & \\ \Phi_G^F(z) &= T_R \cdot V_G^F(z) & \Phi_G^G(z) &= N_c \cdot V_G^G(z). & \end{aligned} \quad (4.38)$$

The splitting functions then take the form (Altarelli&Parisi; Dokshitzer, 1977)

$$V_F^F(z) = 2 \frac{1+z^2}{1-z}$$

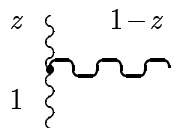
(4.39a)

$$V_F^G(z) = 2 \frac{1+(1-z)^2}{z}$$

(4.39b)

$$V_G^F(z) = 2 [z^2 + (1-z)^2]$$

(4.39c)



$$V_G^G(z) = 4 \left[z(1-z) + \frac{1-z}{z} + \frac{z}{1-z} \right]. \quad (4.39d)$$

The most important symmetry properties of the LLA parton splitting functions are:

Parton Exchange results in an obvious relation between probabilities to find decay products with complementary momenta fractions:

$$V_A^{BC}(z) = V_A^{CB}(1-z). \quad (4.40)$$

A Crossing Relation (Bukhvostov, Lipatov & Popov, 1975) emerges when one links together two splitting processes corresponding to opposite evolution “time” sequences:

$$V_A^B\left(\frac{1}{z}\right) = (-1)^{2s_A+2s_B-1} \frac{1}{z} V_B^A(z) \quad (4.41)$$

with s_A the spin of the particle A .

The Super-Symmetry Relation (Dokshitzer, 1977) exploits the existence of the super-symmetric field theory closely related to real QCD:

$$V_F^F(z) + V_F^G(z) = V_G^F(z) + V_G^G(z). \quad (4.42)$$

Conformal Invariance (Bukhvostov et al., 1985) of the leading twist approximation leads to a number of relations between splitting functions, the simplest of which reads

$$\left(z \frac{d}{dz} - 2\right) V_G^F(z) = \left(z \frac{d}{dz} + 1\right) V_F^G(z). \quad (4.43)$$

As we see, these relations leave not much freedom for splitting functions. In fact, one could borrow V_F^F from a QED text book and reconstruct successively V_F^G (with use of (4.40)), V_G^F (4.41), and then even the gluon selfinteraction V_G^G from (4.42).

The general character of the symmetry properties makes them practically useful when studying next-to-leading corrections to anomalous dimensions and coefficient functions where one faces technically difficult calculations. For example, the super-symmetric QCD analog had been used to choose between two contradictory calculations for the two-loop anomalous dimensions see, e.g. (Altarelli, 1982). We illustrate the idea by another example of the next-to-leading result, e.g. the ratio of parton multiplicities in gluon and quark jets which reads

(Gaffney&Mueller, 1985)

$$R \frac{\mathcal{N}_g}{\mathcal{N}_q} = 1 - \frac{\gamma_0}{6} \{1 + T(1 - 2R)\} + \frac{1}{8} \left(\frac{\gamma_0}{6}\right)^2 \{-25(58R - 19)T + (6 - 4R - 16R^2)T^2\} \quad (4.44)$$

with $\gamma_0 = \sqrt{2N_c\alpha_s/\pi}$ the characteristic PT expansion parameter. R and T in (4.44) are the following ratios of the colour factors:

$$R \equiv \frac{C_F}{N_c}, \quad T \equiv \frac{2n_f T_R}{N_c}.$$

In *susy-QCD* “quark” and “gluon” belong to the same (adjoint) representation of the color group, so that all color factors (4.38) become equal: $C_F = N_c = T_R$. Moreover, the “quark” here is the Majorana fermion (identical to the “antiquark”), so that the total number of $q\bar{q}$ flavor states becomes $2n_f = 1$. Then, as one can easily check, all corrections to the multiplicity ratio $\mathcal{N}_g/\mathcal{N}_q = 1$ in (4.44) vanish at $R = T = 1$.

4.3.2. Space-like parton evolution

The decay phase space for the *space-like* evolution determining the DIS structure functions is

$$dw^{A \rightarrow B+C} = \frac{dk_{\perp}^2}{k_{\perp}^2} \frac{\alpha_s(k_{\perp}^2)}{2\pi} \frac{dz}{z} \Phi_A^{BC}(z) \quad (4.45a)$$

with z the longitudinal momentum fraction carried by the offspring parton B .

In the DIS environment the initial parton A with a negative (space-like) virtuality decays into $B[z]$ with the large space-like virtual momentum $|k_B^2| \gg |k_A^2|$ and a positive virtuality (time-like) $C[1-z]$. The parton C generates a subset of secondary partons (\rightarrow hadrons) in the final state. As long as the process is inclusive, that is that no details of the final-state structure are measured, integration over the subset mass is due, dominated in LLA by the region $k_C^2 \ll |k_B^2|$. The latter condition makes C look *quasi-real*, compared with the hard scale of $|k_B^2|$. The same is true for the initial parton A .

Splitting can be viewed as a large momentum-transfer process of scattering (turnover) of a “real” target parton A into a “real” C on the external field mediated by high-virtuality B . At the next step of evolution it is B ’s turn to play a role of a next target $B \equiv A'$, “real” with respect to yet deeper probe $|k_B'^2| \gg |k_B^2|$, and so on.

Successive parton decays with step-by-step *increasing* space-like virtualities (transverse momenta) constitute the picture of parton wavefunction fluctuations inside the proton. The sequence proceeds until the overall hardness scale Q^2 is reached.

4.3.3. *Time-like parton cascades*

A similar picture emerges for the time-like branching processes determining the internal structure of jets produced, for example, in e^+e^- annihilation. Here the flow of *hardness* is opposite to that in DIS: evolution starts from a highly virtual quark with positive virtuality, originating from the e.m. vertex, while time-like virtualities of its products (“quasi-real” with respect to predecessors; “high-virtuality” with respect to offspring) degrade.

It is important to notice, however, that the flow of *energy* (longitudinal momentum) is governed, in the LLA, by the same functions Φ_A^{BC} : it does not matter that now, in contrast to space-like evolution, A is the “virtual” one and B and C are “real”.

In the time-like case the longitudinal phase space is symmetric in offspring parton energy fractions, and the differential decay probability reads

$$dw^{A \rightarrow B+C} = \frac{d\Theta^2}{\Theta^2} \frac{\alpha_s(k_\perp^2)}{2\pi} dz \Phi_A^{BC}(z). \quad (4.45b)$$

4.3.4. *Fluctuation Time and Evolution Times: Coherence*

An attentive reader has noticed that we wrote the phase space differently: for the space-like case (4.45a) in terms of transverse momentum k_\perp and for the time-like evolution (4.45b) via the decay angle Θ . Logarithmic differentials by themselves are identical, since k_\perp^2 and Θ^2 are proportional for fixed z . We have made this distinction to stress an important difference between a probabilistic interpretation of DIS and the e^+e^- evolution: the different *evolution times*.

An appearance of the angle as a proper evolution parameter in (4.45b) is readily understood: it is a consequence of the Angular Ordering. In the DIS case, (4.45a) we aim at describing, in probabilistic terms, the inclusive cross section, a quantity that could not care less about the finite-state structure and that of soft accompaniment in particular.

To be honest, within the LLA framework it does not make much sense to argue which of evolution parameters $\ln k_{\perp i}^2$, $\ln \Theta_i^2$ or $\ln |k_i^2|$ (with k^2 the total parton virtuality) does a better job: these choices differ by *subleading* terms formally negligible from the LLA point of view. A mismatch is of the order of

$$\sim \alpha_s \ln^2 x. \quad (4.46)$$

It becomes significant, however, and should be “resummed” when numerically small values of the Bjorken x are concerned.⁴

The k_{\perp} -ordering proves to be the one that takes care of potentially disturbing corrections (4.46) in all orders, and in this sense becomes a preferable choice for constructing the probabilistic scheme for single-inclusive parton distributions in DIS.

It is instructive to see how this comes about.

Let us introduce two light-like vectors p_1^{μ} , p_2^{μ} and write down the Sudakov (light-cone) decomposition of momenta:

$$k^{\mu} = \beta p_1^{\mu} + \alpha p_2^{\mu} + k_{\perp}^{\mu}. \quad (4.47)$$

For $k_1^{\mu} + k_2^{\mu} + k_3^{\mu} = 0$ the general relation holds:

$$\frac{k_1^2}{\beta_1} + \frac{k_2^2}{\beta_2} + \frac{k_3^2}{\beta_3} = \frac{\beta_1 \beta_2}{\beta_3} \left(\frac{\vec{k}_{1\perp}}{\beta_1} - \frac{\vec{k}_{2\perp}}{\beta_2} \right)^2. \quad (4.48)$$

Each parton cell in Fig. 12 involves a space-like parton A decaying into $B[z] + C[1-z]$. Relation (4.48) applied to our basic space-like splitting $A \rightarrow B[z]C[1-z]$ gives

$$\frac{-k_B^2}{z} = \frac{-k_A^2}{1} + \frac{k_C^2}{1-z} + \frac{k_{\perp}^2}{z(1-z)}, \quad (4.49)$$

with z the longitudinal momentum fraction — the ratio of the Sudakov light-cone variables β . (We have chosen the direction of p_1 such that $\vec{k}_{A\perp} = 0$, so that $\vec{k}_{B\perp} = -\vec{k}_{C\perp} \equiv \vec{k}_{\perp}$ is the relative transverse momentum in the splitting.)

Since the 4-momenta of A and B are space-like, all terms in (4.49) are positive. B being an intermediate virtual state, k_B^2 enters in the Feynman denominators in the matrix element. The collinear-log contribution arises upon integration over k_{\perp}^2 , over the region where the last term dominates in the r.h.s. of (4.49), that is from the region

$$\frac{|k_B^2|}{z} \simeq \frac{k_{\perp}^2}{z(1-z)} \gg |k_A^2|, \frac{k_C^2}{1-z}. \quad (4.50)$$

The physical origin of this strong inequality becomes transparent in terms of lifetimes of virtual states

$$\tau_i = \frac{k_i^0}{|k_i^2|}, \quad (4.51)$$

⁴ The word “numerically” stands here as a warning for not confusing this kinematical region with a “parametrically” small x , such that $\alpha_s \ln 1/x \sim 1$ — the Regge region — where essentially different physics comes onto stage.

namely $\tau_B \ll \tau_A, \tau_C$. This shows that the LLA contributions originate from the sequence of branchings well separated in the *fluctuation time* (4.51). Invoking the local-scattering analogy (recall $A \rightarrow C$ on the “external field” B), we can say that the classical picture naturally implies “fast scattering”: probing time τ_B much smaller than the lifetime(s) of the “target” before (τ_A) and after the scattering occurs (τ_C).

Assembling a “ladder” of successive parton splittings $i = 1, 2, \dots, n$, and tracing the space-like parton state the n^{th} -order LLA contribution $\sim [\alpha_s \ln(Q^2/\mu^2)]^n$ is expected to come from time-ordered kinematics

$$\frac{P}{\mu^2} \gg \tau_1 \gg \tau_2 \gg \dots \gg \tau_n \gg \frac{xP}{Q^2}.$$

Let us now dig into the k_{\perp}^2 against Θ^2 problem. Equation (4.50) relates virtuality and transverse momentum of the “ t -channel” parton after the i^{th} splitting with the relative longitudinal momentum (β -) fraction z_i :

$$|k_i^2| \simeq \frac{k_{i\perp}^2}{1 - z_i} \approx k_{i\perp}^2. \quad (4.52)$$

The latter approximation is made by remembering that, because of cancellation between real and virtual contributions in inclusive parton distributions (DIS structure functions), the soft s -channel radiation $1 - z_i \ll 1$ does not matter (as long as we stay away from the quasi-elastic kinematics, $1 - x \ll 1$, where it does).

The two-dimensional emission angle (the angle between C and A) can be written and estimated as (cf. (4.48))

$$\bar{\Theta}_i = \frac{\vec{k}_{C\perp}}{\beta_C P} - \frac{\vec{k}_{A\perp}}{\beta_A P} = \frac{\vec{k}_{i-1\perp} - \vec{k}_{i\perp}}{\beta_{i-1}(1 - z_i)P} - \frac{\vec{k}_{i-1\perp}}{\beta_{i-1}P} \approx -\frac{\vec{k}_{i\perp}}{\beta_{i-1}P}. \quad (4.53)$$

We are now in a position to compare different orderings. It is straightforward to get

$$\text{Fluctuation times} \implies k_{i\perp}^2 \gg z_i \cdot k_{i-1\perp}^2, \quad (4.54a)$$

$$\text{Emission angles} \implies k_{i\perp}^2 \gg z_{i-1}^2 \cdot k_{i-1\perp}^2, \quad (4.54b)$$

to be compared with

$$\text{Transverse momenta} \implies k_{i\perp}^2 \gg k_{i-1\perp}^2. \quad (4.54c)$$

For $x = z_1 \cdot z_2 \cdot \dots \cdot z_n \sim 1$ prescriptions (4.54) are essentially equivalent since each decay fraction stays finite, $z_i \sim 1$, and may be neglected in the logarithmic integral over $k_{i\perp}^2$.

For small x , however, the Bethe-Heitler mechanism of DIS off sea quarks dominates (see Fig. 12b). The multi-gluon “ladders” provide

longitudinally enhanced contributions $\propto \ln z_i$, which combine with the $\ln z_i$ factors from the collinear-integration phase space to produce, at the end of the day, the “DL” mismatch $[\alpha_s \ln^2 x]^{n-2}$ between the different options (4.54).

So, which one of the possible orderings (4.54) is correct? The first two prescriptions are more liberal than the last one: they both allow for *disordered* transverse momentum configurations. For example, the fluctuation-time ordering (4.54a) embodies the region

$$z_i \cdot k_{i-1\perp}^2 \ll k_{i\perp}^2 \ll k_{i-1\perp}^2, \quad (4.55)$$

which may be quite broad for $z_i \ll 1$ and where the k_\perp -ordering is violated. The truth is, this region does not contribute to the answer, so that the k_\perp -ordering (4.54c) proves to be the correct one. The reason is quantum mechanical coherence.

4.3.5. Vanishing of the forward inelastic diffraction

Consider a two-step process shown by the first graph in Fig. 13. Let the second decay be *soft* in the t -channel direction, that is $z_2 = \beta_2/\beta_1 \ll 1$. (The first one can be either soft, $z_1 = \beta_1/\beta_0 \ll 1$ or hard, $z_1 \sim 1$.) In the kinematical region (4.55),

$$z_2 \cdot k_{1\perp}^2 \ll k_{2\perp}^2 \ll k_{1\perp}^2, \quad (4.56)$$

the *time-ordering* is still intact, which means that the momentum k_2 is transferred fast as compared with the lifetime of the first fluctuation $P \rightarrow P' + k_1$.

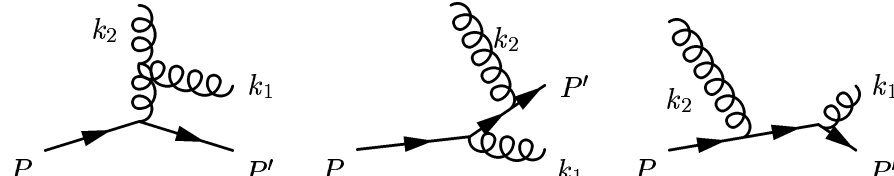


Figure 13. In the “wrong” kinematics $k_{2\perp} < k_{1\perp}$, the sum of the two space-like evolution amplitudes cancels against the final state time-like decay

Since β_2 is small, the process can be viewed as inelastic relativistic scattering $P \rightarrow P' + k_1$ in the external gluon field. The transverse size of the field is $\rho_\perp \sim k_{2\perp}^{-1}$. The characteristic size of the fluctuation $P' + k_1$, according to (4.56), is smaller: $\Delta r_{01\perp} \sim k_{1\perp}^{-1} \ll \rho_\perp$. We thus have a *compact* state propagating through the field that is smooth at distances of the order of the size of the system. In such circumstances the field cannot resolve the internal structure of the fluctuation. Components of the fluctuation, partons P' and k_1 in the first two graphs of Fig. 13, scatter *coherently* with the total amplitude identical and

opposite in sign to that for scattering of the initial state P (the last graph): inelastic breakup does not occur.

This general physical phenomenon is due to Gribov, who has proved that the diffractive deuteron disintegration process vanishes in the forward kinematics. He then used this observation to argue in favour of the so-called weak-Reggeon-coupling regime based on the vanishing of inelastic processes in the $k_{\perp} \rightarrow 0$ limit. In our context the cancellation between the amplitudes of Fig. 13 in the region (4.56) is a direct consequence of the conservation of the colour current.

4.4. HUMPBACED PLATEAU AND LPHD

QCD coherence is crucial for treating particle multiplication **inside** jets, as well as for hadron flows **in-between** jets.

Here we are going to derive together the QCD “prediction” of the inclusive energy spectrum of relatively soft particles from QCD jets. I put the word *prediction* in quotation marks on purpose. This is a good example to illustrate the problem of filling the gap between the QCD formulae, talking quarks and gluons, and phenomena dealing, obviously, with hadrons.

Let me first make a statement:

It is QCD coherence that allows the prediction of the inclusive soft particle yield in jets practically from the “first principles”.

4.4.1. Solving the DIS evolution

You have all the reasons to feel suspicious about this. Indeed, we have stressed above the similarity between the dynamics of the evolution of space-like (DIS structure functions) and time-like systems (jets). On the other hand, you are definitely aware of the fact that the DIS structure functions cannot be calculated perturbatively. There are input parton distributions for the target proton, which have to be plugged in as an initial condition for the evolution at some finite hardness scale $Q_0 = \mathcal{O}(1 \text{ GeV})$. These initial distributions cannot be calculated “from first principles” nowadays but are subject to fitting. What pQCD controls then, is the scaling violation pattern. Namely, it tells us how the parton densities change with the changing scale of the transverse-momentum probe:

$$\frac{\partial}{\partial \ln k_{\perp}} D(x, k_{\perp}) = \frac{\alpha_s(k_{\perp})}{\pi} \int_x^1 \frac{dz}{z} P(z) D\left(\frac{x}{z}, k_{\perp}\right). \quad (4.57)$$

It is convenient to present our “wavefunction” D and “Hamiltonian” P in terms of the complex moment ω , which is Mellin conjugate to the

momentum fraction x :

$$D_\omega = \int_0^1 dx x^\omega \cdot D(x), \quad D(x) = x^{-1} \int_{(\Gamma)} \frac{d\omega}{2\pi i} x^{-\omega} \cdot D_\omega; \quad (4.58a)$$

$$P_\omega = \int_0^1 dz z^\omega \cdot P(z), \quad P(z) = z^{-1} \int_{(\Gamma)} \frac{d\omega}{2\pi i} z^{-\omega} \cdot P_\omega, \quad (4.58b)$$

where the contour Γ runs parallel to the imaginary axis, to the right from singularities of D_ω (P_ω). It is like trading the coordinate ($\ln x$) for the momentum (ω) in a Schrödinger equation.

Substituting (4.58) into (4.57) we see that the evolution equation becomes algebraic and describes propagation in “time” $dt = \frac{\alpha_s}{\pi} d \ln k_\perp$ of a free quantum mechanical “particle” with momentum ω and the dispersion law $E(\omega) = P_\omega$:

$$d D_\omega(k_\perp) = \frac{\alpha_s(k_\perp)}{\pi} \cdot P_\omega D_\omega(k_\perp); \quad \hat{d} \equiv \frac{\partial}{\partial \ln k_\perp}. \quad (4.59)$$

To continue the analogy, our wavefunction D is in fact a multi-component object. It embodies the distributions of valence quarks, gluons and secondary sea quarks which evolve and mix according to the 2×2 matrix LLA “Hamiltonian” Φ_A^B .

At small x , however, the picture simplifies. Here the valence distribution is negligible, $\mathcal{O}(x)$, while the gluon and sea quark components form a system of two coupled oscillators which is easy to diagonalise. What matters is one of the two energy eigenvalues (one of the two branches of the dispersion rule) that is *singular* at $\omega = 0$. The problem becomes essentially one-dimensional. Sea quarks are driven by the gluon distribution while the latter is dominated by gluon cascades. Correspondingly, the leading energy branch is determined by gluon-gluon splitting $g \rightarrow gg$, with a subleading correction coming from the $g \rightarrow q(\bar{q}) \rightarrow g$ transitions,

$$P_\omega = \frac{2N_c}{\omega} - a + \mathcal{O}(\omega), \quad a = \frac{11N_c}{6} + \frac{n_f}{3N_c^2}. \quad (4.60)$$

The solution of (4.59) is straightforward:

$$D_\omega(k_\perp) = D_\omega(Q_0) \cdot \exp \left\{ \int_{Q_0}^{k_\perp} \frac{dk}{k} \gamma_\omega(\alpha_s(k)) \right\}, \quad (4.61a)$$

$$\gamma_\omega(\alpha_s) = \frac{\alpha_s}{\pi} P_\omega. \quad (4.61b)$$

The structure (4.61a) is of the most general nature. It follows from *renormalisability* of the theory, and does not rely on the LLA which

we used to derive it. The function $\gamma(\alpha_s)$ is known as the “anomalous dimension”.⁵ It can be perfected by including higher orders of the PT expansion. Actually, modern analyses of scaling violation are based on the improved next-to-LLA (two-loop) anomalous dimension, which includes α_s^2 corrections to the LLA expression (4.61b).

The structure (4.61a) of the x -moments of parton distributions (DIS structure functions) gives an example of a clever separation of PT and NP effects; in this particular case — in the form of two factors. It is the ω -dependence of the input function $D_\omega(Q_0)$ (“initial parton distributions”) that limits predictability of the Bjorken- x dependence of DIS cross sections.

So, how comes then that in the time-like channel the PT answer turns out to be more robust?

4.4.2. Coherent hump in $e^+e^- \rightarrow h(x) + \dots$

We are ready to discuss the time-like case, with $D_j^h(x, Q)$ now the inclusive distribution of particles h with the energy fraction (Feynman- x) $x \ll 1$ from a jet (parton j) produced at a large hardness scale Q .

Here the general structure (4.61a) still holds. We need, however, to revisit the expression (4.61b) for the anomalous dimension because, as we have learned, the proper evolution time is now different from the case of DIS.

In the time-like jet evolution, due to Angular Ordering, the evolution equation becomes non-local in k_\perp space:

$$\frac{\partial}{\partial \ln k_\perp} D(x, k_\perp) = \frac{\alpha_s(k_\perp)}{\pi} \int_x^1 \frac{dz}{z} P(z) D\left(\frac{x}{z}, z \cdot k_\perp\right). \quad (4.62)$$

Indeed, successive parton splittings are ordered according to

$$\theta = \frac{k_\perp}{k_\parallel} > \theta' = \frac{k'_\perp}{k'_\parallel}.$$

Differentiating $D(k_\perp)$ over the scale of the “probe”, k_\perp , results then in the substitution

$$k'_\perp = \frac{k'_\parallel}{k_\parallel} \cdot k_\perp \equiv z \cdot k_\perp$$

in the argument of the distribution of the next generation $D(k'_\perp)$.

⁵ The name is a relict of those good old days when particle and solid state physicists used to have common theory seminars. If the coupling α_s were constant (had a “fixed point”), then (4.61a) would produce the function with a non-integer (non-canonical) dimension $D(Q) \propto Q^\gamma$ (analogy — critical indices of thermodynamical functions near the phase transition point).

The evolution equation (4.62) can be elegantly cracked using the Taylor-expansion trick,

$$D(z \cdot k_{\perp}) = \exp \left\{ \ln z \frac{\partial}{\partial \ln k_{\perp}} \right\} D(k_{\perp}) = z^{\frac{\partial}{\partial \ln k_{\perp}}} \cdot D(k_{\perp}). \quad (4.63)$$

Turning as before to moment space (4.58), we observe that the solution comes out similar to that for DIS, (4.61), but for one detail. The exponent \hat{d} of the additional z -factor in (4.63) combines with the Mellin moment ω to make the argument of the splitting function P a *differential operator* rather than a complex number:

$$\hat{d} \cdot D_{\omega} = \frac{\alpha_s}{\pi} P_{\omega+\hat{d}} \cdot D_{\omega}. \quad (4.64)$$

This leads to the differential equation

$$\left(P_{\omega+\hat{d}}^{-1} \hat{d} - \frac{\alpha_s}{\pi} - \left[P_{\omega+\hat{d}}^{-1}, \frac{\alpha_s}{\pi} \right] P_{\omega+\hat{d}} \right) \cdot D = 0. \quad (4.65)$$

Recall that, since we are interested in the small- x region, the essential moments are small, $\omega \ll 1$.

For the sake of illustration, let us keep only the most singular piece in the “dispersion law” (4.60) and neglect the commutator term in (4.65) generating a subleading correction $\propto \hat{d}\alpha_s \sim \alpha_s^2$. In this approximation (DLA),

$$P_{\omega} \simeq \frac{2N_c}{\omega}, \quad (4.66)$$

(4.65) immediately gives a quadratic equation for the anomalous dimension,⁶

$$(\omega + \gamma_{\omega})\gamma_{\omega} - \frac{2N_c\alpha_s}{\pi} + \mathcal{O}\left(\frac{\alpha_s^2}{\omega}\right) = 0. \quad (4.67)$$

The leading anomalous dimension following from (4.67) is

$$\gamma_{\omega} = \frac{\omega}{2} \left(-1 + \sqrt{1 + \frac{8N_c\alpha_s}{\pi\omega^2}} \right). \quad (4.68)$$

When expanded to first order in α_s , it coincides with that for the space-like evolution, $\gamma_{\omega} \simeq \alpha_s/\pi \cdot P_{\omega}$, with P given in (4.66). Such an expansion, however, fails when characteristic $\omega \sim 1/|\ln x|$ becomes as small as $\sqrt{\alpha_s}$, that is when

$$\frac{8N_c\alpha_s}{\pi} \ln^2 x \gtrsim 1.$$

⁶ It suffices to use the next-to-leading approximation to the splitting function (4.60) and to keep the subleading correction coming from differentiation of the running coupling in (4.65) to get the more accurate MLLA anomalous dimension γ_{ω} .

This inequality is an elaboration of the heuristic estimate (4.46).

Now what remains to be done is to substitute our new weird anomalous dimension into (4.61a) and perform the inverse Mellin transform to find $D(x)$. If there were no QCD parton cascading, we would expect the particle *density* $xD(x)$ to be constant (Feynman plateau). It is straightforward to derive that plugging in the DLA anomalous dimension (4.68) results in the plateau density increasing with Q and with a maximum (hump) “midway” between the smallest and the highest parton energies, namely, at $x_{\max} \simeq \sqrt{Q_0/Q}$. The subleading MLLA effects shift the hump to smaller parton energies,

$$\ln \frac{1}{x_{\max}} = \ln \frac{Q}{Q_0} \left(\frac{1}{2} + c \cdot \sqrt{\alpha_s} + \dots \right) \simeq 0.65 \ln \frac{Q}{Q_0},$$

with c a known analytically calculated number. Moreover, defying naive probabilistic intuition, the softest particles do not multiply at all. The density of particles (partons) with $x \sim Q_0/Q$ stays constant while that of their more energetic companions increases with the hardness of the process Q .

This is a powerful legitimate consequence of pQCD coherence. We turn now to another, no less powerful though less legitimate, consequence.

4.4.3. Coherent damping of the Landau singularity

The time-like DLA anomalous dimension (4.68), as well as its MLLA improved version, has a curious property. Namely, in sharp contrast with DIS, it allows the momentum integral in (4.61) to be extended to very small scales. Even integrating down to $Q_0 = \Lambda$, the position of the “Landau pole” in the coupling, one gets a finite answer for the distribution (the so-called *limiting spectrum*), simply because the $\sqrt{\alpha_s(k)}$ singularity happens to be integrable!

It would have been poor taste to trust this formal integrability, since the very PT approach to the problem (selection of dominant contributions, parton evolution picture, etc.) relied on α_s being a numerically small parameter. However, the important thing is that, due to time-like coherence effects, the (still perturbative but “smallish”) scales, where $\alpha_s(k) \gg \omega^2$, contribute to γ basically in a ω -independent way, $\gamma + \omega/2 \propto \sqrt{\alpha_s(k)} \neq f(\omega)$. This means that “smallish” momentum scales k affect only an overall *normalization* without affecting the *shape* of the x -distribution.

Since this is the rôle of the “smallish” scales, it is natural to expect the same for the truly small — non-perturbative — scales where the partons transform into the final hadrons. This hypothesis (LPHD) reduces, mathematically, to the statement (guess) that the NP factor in

(4.61a) has a finite $\omega \rightarrow 0$ limit:

$$D_{\omega}^{(h)}(Q_0) \rightarrow K^h = \text{const}, \quad \omega \rightarrow 0.$$

Thus, according to LPHD, the x -shape of the so-called “limiting” parton spectrum which is obtained by formally setting $Q_0 = \Lambda$ in the evolution equations, should be mathematically similar to that of the inclusive distribution of *hadrons* (h). Another essential property is that the “conversion coefficient” K^h should be a true constant independent of the hardness of the process producing the jet under consideration.

References

- Altarelli, G., Phys.Rep. 81 (1982) 1.
 Altarelli, G. and G. Parisi, Nucl.Phys. B 126 (1977) 298.
 Abreu, P. et al., DELPHI Collab., Phys.Lett. B 449 (1999) 383; Eur.Phys.J. C 13 (2000) 573.
 Akers, R. et al., OPAL Collab., Z.Phys. C 68 (1995) 531.
 Azimov, Ya.I., Yu.L. Dokshitzer, V.A. Khoze and S.I. Troyan, Phys.Lett. 165 B (1985) 147.
 Bukhvostov, A.P., L.N. Lipatov and N.P. Popov, Sov.J.Nucl.Phys. 20 (1975) 287.
 Bukhvostov, A.P., G.V. Frolov, L.N. Lipatov and E.A. Kuraev. Nucl.Phys. B 258 (1985) 601.
 Camici, G. and M. Ciafaloni, Phys.Lett. B 395 (1997) 118.
 DELPHI Collab., K. Hamacher et al., submitted to EPS-HEP Conference, Tampere, Finland, June 15, 1999; contribution 1-145.
 Dokshitzer, Yu.L., Sov.Phys.JETP 46 (1977) 641.
 Dokshitzer, Yu.L. and S.I. Troyan, “Asymptotic Freedom and Local Parton-Hadron Duality in QCD Jet Physics”. In *Proceedings of 19th Leningrad Winter School* (in Russian), vol. 1, p. 144, Leningrad 1984;
 Ya.I. Azimov et al., Z.Phys. C 27 (1985) 65;
 Yu.L. Dokshitzer, V.A. Khoze, A.H. Mueller and S.I. Troyan, *Basics of Perturbative QCD* (ed. J. Tran Thanh Van) Gif-sur-Yvette, Editions Frontières, 1991.
 Dokshitzer, Yu.L., V.A. Khoze, A.H. Mueller and S.I. Troyan, Rev.Mod.Phys. 60 (1988) 373.
 Fong, C.P. and B.R. Webber, Nucl.Phys. B 355 (1991) 54.
 Gaffney, J.B. and A.H. Mueller, Nucl.Phys. B 250 (1985) 109.
 Goulianos, D., CDF Collab., In *Proceedings 32nd Recontres de Moriond*, Les Arcs, France, March 22, 1997.
 Hamacher, K., O. Klapp, P. Langefeld and M. Siebel, DELPHI Collab., submitted to EPS-HEP Conference, Tampere, Finland, June 15, 1999; contribution 1-571.
 Hoyer, P., N. Marchal and S. Peigne, Phys.Rev. D 62 (2000) 114001
 Khoze, V.A., S. Lupia and W. Ochs, Phys.Lett. B 394 (1997) 179.
 Korytov, A., 1996, private communication.
 Mueller, A.H., Nucl.Phys. B 213 (1983) 85. Erratum quoted *ibid.*, B 241 (1984) 141.
 Mueller, A.H., Phys.Lett. B 396 (1997) 251.
 Safonov, A.N., CDF Collab., In *Proceedings International Euroconference in Quantum Chromodynamics*, Montpellier, France, July 7, 1999.

